131 Hartwell Avenue
Lexington, Massachusetts
02421-3126
USA
Tel: +1 781 761-2288
Fax: +1 781 761-2299
www.aer.com

FINAL REPORT

Assessment of the Exceptional Event Rule's 'Q/D' Guidance

TCEQ Contract No. 582-15-50414
Work Order No. 582-18-81899-09
Revision 2.0

Prepared by:
Benjamin Brown-Steiner, Chantelle Lonsdale, Jennifer Hegarty, and Matthew Alvarado
Atmospheric and Environmental Research, Inc. (AER)
131 Hartwell Ave.
Lexington, MA 02466

Correspondence to: malvarad@aer.com

Prepared for:
Erik Gribbin
Texas Commission on Environmental Quality
Air Quality Division
Building E, Room 342S
Austin, TX 78711-3087

June 29, 2018

Document Change Record

Revision	Revision Date	Remarks
0.1	29 May 2018	Internal Version for Review
1.0	1 June 2018	Draft Submitted to the TCEQ
2.0	29 June 2018	Final Report After Comments from the TCEQ

TABLE OF CONTENTS

List of Figures

List of Tables

List of Acronyms

AER – Atmospheric and Environmental Research
ASP – Aerosol Simulation Program
CAMx – Comprehensive Air Quality Model with Extensions
CMAQ – Community Multiscale Air Quality Modeling System
CO – Carbon Monoxide
ΔCO – Change in Carbon Monoxide
CST – Central Standard Time
CSV – Comma Separated Value
D - Distance
DFW – Dallas/Fort Worth
EER – Exceptional Event Rule
EPA – Environmental Protection Agency
FINN – Fire Inventory from NCAR
g – Earth's gravitational constant
GAM – Generalized Additive Model
HGB – Houston/Galveston/Brazoria
HNO_3 – Nitric Acid
HONO – Nitrous Acid
hr - hour
HYSPLIT – Hybrid Single Particle Lagrangian Integrated Trajectory
IVOC (S/IVOC)
kg - kilogram
km - kilometer
m - meter
MDA8 – Maximum Daily 8-hour Average
MEGAN – Model of Emissions of Gases and Aerosols from Nature
mol - molecule
MOS – Model Output Statistics
NAAQS – National Ambient Air Quality Standards
NAM – North American Mesoscale forecast system
NARR – North American Regional Reanalysis
NCAR – National Center for Atmospheric Research
NCEP – National Centers for Environmental Prediction
NEI – National Emissions Inventory
NH_3 - Ammonia

NMOCs – Non-Methane Organic Compounds
NO_x – Nitrogen Oxide
NO_y – Reactive Nitrogen ($NO_x + N_2O_5 + HNO_3$)
O_3 – Ozone
OH – Hydroxyl Radical
$PM_{2.5}$ – Particulate Metter (smaller than 2.5 microns)
rNRT – near-real-time
PAN – Peroxyacetyl Nitrate
ppbv – parts per billion by volume
Q – Sum of emissions of VOCs and NOx
QAPP – Quality Assurance Project Plan
Q/D – "Q over D", the ratio of wildfire emissions ($rVOC + NO_x = Q$) to distance (D)
ROC – Relative Operating Characteristic
SA – San Antonio
SmartFire – Satellite Mapping Automated Reanalysis Tool for Fire Incident Reconciliation
SOA – Secondary Organic Aerosols
STILT-ASP – Stochastic Time Inverted Lagrangian Transport - Aerosol Simulation Program
TCEQ – Texas Commission on Environmental Quality
TOG – Total Organic Gases
tpd – tons per day
TUV – Tropospheric Ultraviolet and Visible
UTC – Coordinated Universal Time
UTEP – University of Texas at El Paso
VOC – Volatile Organic Compound
WRF – Weather Research and Forecasting

Executive Summary

The purpose of this project was to create a technical assessment of the "Q/D" criteria developed by the US EPA as part of guidance for its Exceptional Events Rule (EER). The EER determines how the US EPA uses or treats air quality monitoring data influenced by exceptional events. The rule determines the conditions under which the US EPA will forgo comparison of policy relevant air monitoring data to a relevant National Ambient Air Quality Standard (NAAQS).

In Task 2 of this project, we reviewed the evidence provided by EPA for the validity of the Q/D screening metric for the O_3 impacts of wildfires. In Task 3, we reviewed the literature on the formation of O_3 in biomass burning plumes and analyze the observations for their consistency with the Q/D screening metric. In Tasks 4 and 5, AER used the ASP and STILT-ASP models to simulate the O_3 formation in biomass burning plumes in two events when fires in the Yucatan impacted the Houston/Galveston/Brazoria (HGB) urban area (Task 4) as well as an exceptional event in El Paso, Texas on June 21, 2015 (Task 5). In Task 5, we also analyzed output of the CAMx model (using CAMx inputs and outputs provided by the TCEQ). Previously generated generalized additive models (GAMs) for the HGB urban were also used to quantify the GAM residuals during these events, which have been proposed as another method for identifying biomass burning impacts on O_3. We assessed all model simulations of these events for consistency with the Q/D metric.

The ASP simulations generally show O_3 increasing with time and distance downwind over the two-day time frame simulated, and were thus inconsistent with the Q/D metric. However, the O_3 produced did increase somewhat proportionally with initial emissions if other parameters (e.g., mixing height, fire area) are held constant. While the O_3 formation at the end of two days is similar for fires with similar initial CO concentrations from grassland/savannah, tropical forest, and temperate forest fires, the O_3 formation from boreal forest fires is much lower, suggesting that different metrics are needed for screening O_3 impacts from boreal biomass burning fires.

The STILT-ASP simulations showed O_3 production within individual parcels regularly increased with increasing distance from the wildfire source, while individual parcels behaviors were highly variable in both their trajectory and their O_3 chemistry. Together, our simulations and analysis demonstrate ozone behavior that is largely inconsistent with the Q/D metric. In particular, the wide range of back-trajectory behavior and the variable O_3 chemistry within individual parcels as calculated by STILT-ASP show the limits of the Q/D metric, namely in the assumption that a straight-line distance as a proxy for the travel distance of a parcel and in the assumption that the influence of wildfire emissions on ozone decreases as a function of distance from the wildfire.

Analysis of the CAMx results for the El Paso exceptional event shows that the CAMx-simulated impacts of biomass burning on MDA8 O_3 on this day are not consistent with the Q/D metric. Instead, the fire impacts on MDA8 O_3 tend to increase with distance within 200-300 km of the fire, with some evidence of the Hog fire having additional O_3 production due to interaction with the anthropogenic NO_x in the El Paso-Ciudad Juárez urban area. This dependence on distance is qualitatively consistent with the ASP and STILT-ASP model results.

Using the GAMs for the HGB urban area to estimate fire impacts was not very effective, as the GAM model residuals during these events (+3-4 ppbv) are well within the standard error of the GAMs (~10 ppbv), and thus it is unclear if the residuals are due to fires or simply due to the random errors that are unavoidable in statistical models.

Instead of the Q/D metric, we recommend a literature-based approach that uses literature ratios of O_3 enhancement by fires to the enhancement of CO and/or NO_y in the plumes. STILT-

ASP back-trajectories can be used to estimate the impact of fires on CO and/or NO_y without needing to have the computational expense or complication of calculating the photochemistry. Thus the level of effort required for a Tier 2 demonstration with this approach would not be appreciably larger than what is already required for the Q/D plus back-trajectory approach.

We also recommend that future work on the formation of O_3 in biomass burning plumes and their impacts on urban areas in Texas focus on:

- Using models to separate the O_3 formation within the biomass burning plume itself from the O_3 production caused by the mixing of biomass burning VOCs with anthropogenic NO_x in urban areas.
- Improving the chemistry in 3D Eulerian regional air quality models like CAMx and CMAQ to better represent the chemistry of biomass burning VOCs, including their formation of O_3, organic nitrates, and secondary organic aerosol (SOA).
- Parameterizing O_3 formation in biomass burning plumes using model emulators and other techniques to rapidly estimate the impacts of fires on a given urban area.
- Improvements to the STILT-ASP model, including better representation of plume rise, mixing among parcels, and deposition.

1. Introduction

1.1 Project Objectives

The purpose of this project was to create a technical assessment of the "Q/D" criteria developed by the US EPA as part of guidance for its Exceptional Events Rule (EER). The EER determines how the US EPA uses or treats air quality monitoring data influenced by exceptional events. The rule determines the conditions under which the US EPA will forgo comparison of policy relevant air monitoring data to a relevant National Ambient Air Quality Standard (NAAQS).

In Task 2 of this project, we reviewed the evidence provided by EPA for the validity of the Q/D screening metric for the O_3 impacts of wildfires. In Task 3, we reviewed the literature on the formation of O_3 in biomass burning plumes and analyze the observations for their consistency with the Q/D screening metric.

In Tasks 4 and 5, AER used the ASP and STILT-ASP models to simulate the O_3 formation in biomass burning plumes in two events when fires in the Yucatan impacted the Houston/Galveston/Brazoria (HGB) urban area (Task 4) as well as a potential exceptional event in El Paso, Texas (Task 5). In Task 5, we also analyzed output of the CAMx model (using CAMx inputs and outputs provided by TCEQ). Previously generated generalized additive models (GAMs, Wood, 2006) for the HGB urban areas (Pernak et al., 2017) were also used to quantify the GAM residuals during these events, which have been proposed as another method for identifying biomass burning impacts on O_3 (Gong et al., 2017). We assessed all model simulations of these events for consistency with the Q/D metric. Based on these analyses, we propose other metrics that could be used to quickly assess the impacts of biomass burning on surface O_3 at selected monitors.

The schedule of deliverables for this project is given in Table 1.

Table 1. Projected Schedule for TCEQ Work Order No. 582-18-81899-09

Milestones	Planned Date
Task 1 - Work Plan	
1.1: TCEQ-approved Work Plan	January 19, 2018
1.2: TCEQ-approved QAPP	January 19, 2018
Task 2 - Evaluate EPA documentation and justification of Q/D as a screening tool	
2.1: A revised work plan and QAPP based on the review of the EPA's evidence and discussions with EPA personnel.	March 31, 2018
Task 3 – Literature search on O_3 formation in Biomass Burning Plumes versus the Q/D metric	
3.1: A brief technical memo summarizing the results of the literature search and analysis.	April 30, 2018
Task 4 – Modeling the Impact of Biomass Burning Plumes on Ozone in Houston, Texas Using Multiple Models and Comparing to the Q/D metric	
4.1: Summary of the analyses of the HGB events using ASP and STILT-ASP.	With Final Report due June 30, 2018.
Task 5 – Modeling the Impact of Biomass Burning Plumes on Ozone in El Paso, Texas Using Multiple Models and Comparing to the Q/D metric	
5.1: Summary of the analyses of the El Paso event using CAMx, ASP, and STILT-ASP.	With Final Report due June 30, 2018.
Task 6 – Draft and Final Reports	
6.1: Draft Report	June 1, 2018
6.2: Final Report	June 30, 2018

1.2 Background

On October 3, 2016, the US EPA published its revisions to the EER[1]. Approximately two weeks prior to publishing its EER revisions, the US EPA published final "Guidance on the Preparation of Exceptional Events Demonstrations for Wildfire Events that May Influence Ozone Concentrations" intended to align with the EER revisions. One notable feature of the guidance was the inclusion of tiers to outline the level of technical evidence required in states' EER demonstrations for simple versus more complex events:

[1] "Treatment of Data Influenced by Exceptional Events; Final Rule" (81 FR 68216, October 3, 2016)

> *"This guidance outlines a tiered approach for addressing the clear causal relationship element within a wildfire/ozone demonstration, recognizing that some wildfire events may be more clear and/or extreme and, therefore, require relatively less evidence to satisfy the rule requirements. Tier 1 clear causal analyses should be used for wildfire events that cause clear O_3 impacts in areas or during times of year that typically experience lower O_3 concentrations, and are thus simpler and less resource intensive than analyses for other events. Tier 2 clear causal analyses are likely appropriate when the impacts of the wildfire on O_3 levels are less clear and require more supportive documentation than Tier 1 analyses. Tier 3 clear causal analyses should be used for events in which the relationship between the wildfire and the O_3 exceedance or violation is more complicated than the relationship in a Tier 2 analysis, and thus would require more supportive documentation than Tier 2 analyses. ..." (Geographic Strategies Group, 2016, 4)*

In order to help determine which fire events would be evaluated on Tier 2 versus Tier 3, the EPA introduced the Q/D (emissions/distance) metric to screen events. According to the US EPA (Geographic Studies Group, 2016, 16): *"Examination of this modeling and related studies suggests that it is appropriate to use a simple Q/D (emissions/distance) metric to conduct a screening assessment of potential fire impacts. This model application was evaluated against monitoring data and appears to capture the ambient relationships between CO and O_3 measured in the vicinity of smoke plumes."* Section 3.5.1 includes recommended values for an event's assignment to Tier 2 and suggestions for calculating Q/D (Geographic Strategies Group, 2016, 16-21).

Wildfires can significantly impact ozone (O_3) concentrations far downwind of the fire, either by secondary production of O_3 in the smoke plume, long-range transport of fire VOCs to high NO_x urban areas to increase O_3 production, or long-range transport of peroxyacetyl nitrates to low NO_x regions (where they decompose and increase NO_x concentrations). These O_3 impacts from fires can potentially qualify as exceptional events under the Clean Air Act, but since using photochemical models to demonstrate the level of fire impact on O_3 is very labor intensive, there is a need for a quick metric that can be used to identify potential Tier 2 and Tier 3 exceptional events. Currently, EPA is using a "Q/D" metric for this screening, where the emissions of NO_x and VOCs from a fire (Q) are divided by the distance the monitor is from the fire (D). However, while this would work for a primary emitted pollutant, this metric likely does not capture the non-linear behavior of secondary O_3 production in smoke plumes, where O_3 concentrations near the fire are reduced below background by NO_x titration before increasing downwind. It also does not capture the effects that biomass burning has been shown to have on O_3 concentrations hundreds to thousands of kilometers downwind of the fire.

In this study, AER performed a literature review on the long-range impacts of biomass burning emissions on O_3 to assess the validity of the Q/D metric. AER then performed modeling using the ASP and STILT-ASP Lagrangian transport models to assess the validity of the "Q/D" metric under different burning conditions, as well as to propose other metrics that could be used to quickly assess the impacts of biomass burning on surface O_3 at selected monitors.

1.3 Report Outline

This Final Report highlights major activities and key findings, provides pertinent analysis, describes encountered problems and associated corrective actions, and details relevant statistics

including data, parameter, or model completeness, accuracy and precision. It satisfies Deliverables 4.1, 5.1, and 6.2 of the Work Plan for Work Order No. 582-18-81899-09:

Deliverable 4.1:	Summary of the analyses of the HGB events using ASP and STILT-ASP.
Deliverable 4.1 Due Date:	With Final Report due June 30, 2018
Deliverable 5.1:	Summary of the analyses of the El Paso event using CAMx, ASP, and STILT-ASP.
Deliverable 5.1 Due Date:	With Final Report due June 30, 2018
Deliverable 6.2:	Final Report
Deliverable 6.2 Due Date:	June 30, 2018

Section 2 of this report contains the assessment of the EPA's evidence for the Q/D metric and the results of the literature review. Section 3 summarizes the ASP and STILT-ASP model results for the HGB events and analyzes them for consistency with the Q/D metric. Section 4 summarizes the ASP, STILT-ASP, and CAMx model results for the El Paso event and analyzes them for consistency with the Q/D metric. Section 5 then suggests alternative metrics that could be used to quickly assess the impact of biomass burning on urban area O_3.

Section 6 discusses the Quality Assurance performed for the project, including answers to the assessment questions from the Quality Assurance Project Plan (QAPP). Section 7 summarizes the conclusions of our study and Section 8 gives our recommendations for further research.

2 Literature Review of O_3 Formation in Biomass Burning Plumes

2.1 Assessment of the EPA's Exceptional Event Rule and Guidance Memo

The US EPA's 2016 revision to the 2007 Exceptional Event Rule (40 CFR 50.14(c)(3)) and their September 16, 2016 Guidance Memo updates procedures for demonstrating a "clear causal relationship" between wildfires and exceptional ozone events based on "implementation experiences." The Guidance Memo requires that an exceptional event demonstration include: (1) a narrative model of the wildfire influence on the exceedance; (2) a demonstration of a clear, causal relationship between the wildfire event and the receptor; (3) historical data for the receptor in question; (4) evidence that the event was not "reasonably controllable and not reasonably preventable"; (5) a demonstration that the event was rare or natural; and (6) a demonstration that appropriate public comment rules were followed.

The EPA considers exceptional event demonstrations following a qualitative weight-of-evidence process that includes a three-tiered approach for demonstrating the wildfire influence on ozone exceedances. The Guidance Memo gives direction as to what evidence is required for an exceptional event demonstration for each of the three tiers.

One piece of evidence used during these demonstrations is the Q/D metric, which provides an estimate of the size of the wildfire emission source (Q) and the distance between this source and a receptor (D). The Q/D metric is not needed for Tier 1 demonstrations, which require the least amount of demonstrated evidence, but it is used to determine if a Tier 2 or Tier 3 demonstration is required. If the Q/D value is larger than 100 tons per day per kilometer (tpd/km), indicating a large, nearby wildfire, the demonstration is likely to be of Tier 2. If, however, the Q/D value is less than 100 tpd/km – indicating either a smaller, nearby wildfire or a large, but distant, wildfire – additional evidence is required that meets the more stringent requirements of Tier 3.

The EPA Guidance Memo highlights the utility of the Q/D metric, and in particular the selection of the 100 tpd/km threshold for the identification of regions and times in which the likelihood of wildfire influence on ozone enhancement is high. A threshold of 200 tpd/km tends to identify source regions only, while a threshold of 50 tpd/km tends to overestimate the potential fire impact (e.g. all of the Western and Central US had at least one day with a Q/D over 50 tpd/km during 2012, with much of the Northwestern US having more than 10 days with a Q/D over 50 tpd/km).

The 100 tpd/km threshold allows for the identification of regions likely impacted by the high-fire year 2008 for California and Oregon, and the high-fire year 2012 in Wyoming, Montana, and Idaho, as well as regional high-fire years (e.g. 2009 in Georgia, 2011 in Kansas). However, it should be noted that this 100 tpd/km Q/D metric is only a demonstration of the *potential* for fire emissions to impact O_3. Additional evidence is necessary, including meteorological back-trajectories of the fire emissions and surface observations showing an enhancement of O_3 concurrent with the timing of the arrival of advected fire plumes.

Definition of Q and D and the Calculation of the Q/D Metric

The EPA Guidance Memo describes the procedure for calculating Q/D on pages 17 – 21, and defines Q as:

> *"the daily sum of the NO_x and reactive VOC emissions (in units of tons per day) from specific wildfire events impacting the O_3 monitor on the day of the O_3 exceedance."*

The EPA's approach for estimating Q depends on satellite fire detection methods, surface observations, and models including Satellite Mapping Automated Reanalysis Tool for Fire Incident Reconciliation (SmartFire) and the National Emissions Inventory (NEI), among others.

The EPA Guidance Memo defines D as:

> *"the distance in kilometers between the fire's latitude/longitude and the affected O_3 monitor for each fire for each day."*

This D metric typically is defined at the centroid of each day's fire parcel, but the EPA notes that agencies can use other locations within a fire parcel if "the latitude/longitude calculation is well-documented and supported."

Then, for each fire and each day, the agency should calculate the Q/D "emissions divided by distance" metric. If any fire on any day has a Q/D value that exceeds 100 tpd/km, or if a calculation of the Q/D metric for an aggregation of different fires within a single day can be demonstrated, the agency should proceed to a demonstration that the exceedance event is unusual within the historical data of the O_3 monitor. If that can be demonstrated, then the Tier 2 level of evidence has been met for the exceptional event demonstration. If, however, no single fire event or the aggregate of fire events within a single day exceeds the 100 tpd/km metric, the agency would then have to meet the Tier 3 levels of evidence for their exceptional event demonstration.

The EPA Guidance Memo is clear that the "Q/D screening step alone is not sufficient to delineate conditions where sizeable impacts are likely to occur" and that the Q/D screening threshold of 100 tpd/km is a "conservative value" that will exclude many cases that would be identified as exceptional events under a Tier 3 analysis.

2.2 Q, D and Ozone Enhancement Results from Available Literature

While wildfire emissions emit a wide range of chemical species (e.g. Akagi et al., 2011) we are interested in this literature review particularly in *volatile organic compounds* (VOCs) and *nitrogen oxides* (NO_x). While the NO_x chemical family contains only two species (NO and NO_2), the VOC emissions in biomass burning emission inventories include a large list of species – almost certainly an incomplete list – some of which are close to detection limits (e.g. Andreae and Merlet, 2001; Akagi et al., 2011). Within biomass burning plumes, VOCs typically refer to the sum of non-methane organic compounds (NMOCs) such as alkanes, alkenes, alkynes, terpenes, aromatics, and derivatives, as well as aldehydes, alcohols, ketones, organic acids, and other minor species, although only a few tend to make up most of the VOC mass.

For example, Wentworth et al. (2018) measured the concentrations of 65 VOC species during the 2016 Fort McMurray Wildfire in Canada and found that 6 species made up ~ 97% of the total VOCs: methanol, acetaldehyde, acetone, benzene, 1-butene, and formaldehyde. Wentworth et al. (2018) found that these were consistent with previous studies (Andreae and Merlet, 2001; Urbanski, 2013).

The EPA Guidance Memo defines Q as the sum of NO_x and the sum of the *reactive volatile organic compounds* (rVOCs), but also accepts an estimate of *total organic gases* (TOGs) that can be multiplied by 0.6 to provide an estimate of the rVOCs.

For this review, we will follow the EPA (https://www.epa.gov/indoor-air-quality-iaq/technical-overview-volatile-organic-compounds) recommended definition of VOCs:

> *Any compound of carbon, excluding carbon monoxide, carbon dioxide, carbonic acid, metallic carbides or carbonates and ammonium carbonate, which participates in atmospheric photochemical reactions, except those designated by EPA as having negligible photochemical reactivity...VOCs are organic chemical compounds whose composition makes it possible for them to evaporate under normal indoor atmospheric conditions of temperature and pressure.*

The EPA further classifies VOCs not by a list of species that it contains, but with a list of non-reactive or negligibly reactive compounds that can change over time. Thus the term VOCs is a loose one, but for the purposes of this review, we will include estimates of VOCs if they are identified or classified as rVOCs or TOG in a scientific publication, even if they do not define the specific species included.

Only two of the publications we found in our review that provide estimates if the ozone enhancement from fires also estimate fire emissions directly in a tons-per-day format necessary for estimates of the Q-value (Lei et al., 2013 and Baker et al., 2016). Lei et al. (2013) estimate fires near Mexico City, although Q values are small (less than 400 tons per day) and little ozone enhancement is noted. Baker et al. (2016) estimate Q-values for two fire events in 2011 estimating emissions with the SmartFire version 2 (Raffuse et al., 2012) and BlueSky emissions framework. The Baker et al. (2016) simulations find high ozone enhancement near the Flint Hill and Wallow wildfire sources and non-negligible (< 5 ppbv) ozone enhancement within Texas. Craig et al. (2013) also examined the Flint Hill fire events, finding the impact of the Flint Hills fire over Texas to be small (< 5 ppbv).

We calculate Q values for the same fire days as identified in Baker et al. (2016) and for other fires identified in the literature (below) by utilizing the Fire INventory from NCAR (FINN) database (https://www2.acom.ucar.edu/modeling/finn-fire-inventory-ncar) speciated to the MOZART-4 chemical mechanism. We first convert the FINN data (.csv files) to netCDF files (matching the dates of individual wildfires) gridded to match the 12-kilometer resolution NAM12 meteorological grid. From this gridded dataset we define a latitude-longitude box around the wildfire event and sum up the emissions of all rVOCs (see Appendix Table A1 for a list of rVOC species) and NO_x for each hour in a given day. We include in Appendix Table A2 the latitude/longitude bounds used to define the fires included in this analysis and note that there is some uncertainty in the calculated Q-value based on the definition of this bounding box: a larger box captures more wildfire emissions, but guarantees that all emissions from a wildfire event are captured, perhaps even some from other, smaller wildfires. A smaller box reduces the risk of including additional fire events, but also could potentially exclude wildfire emissions that are actually part of the wildfire event in question.

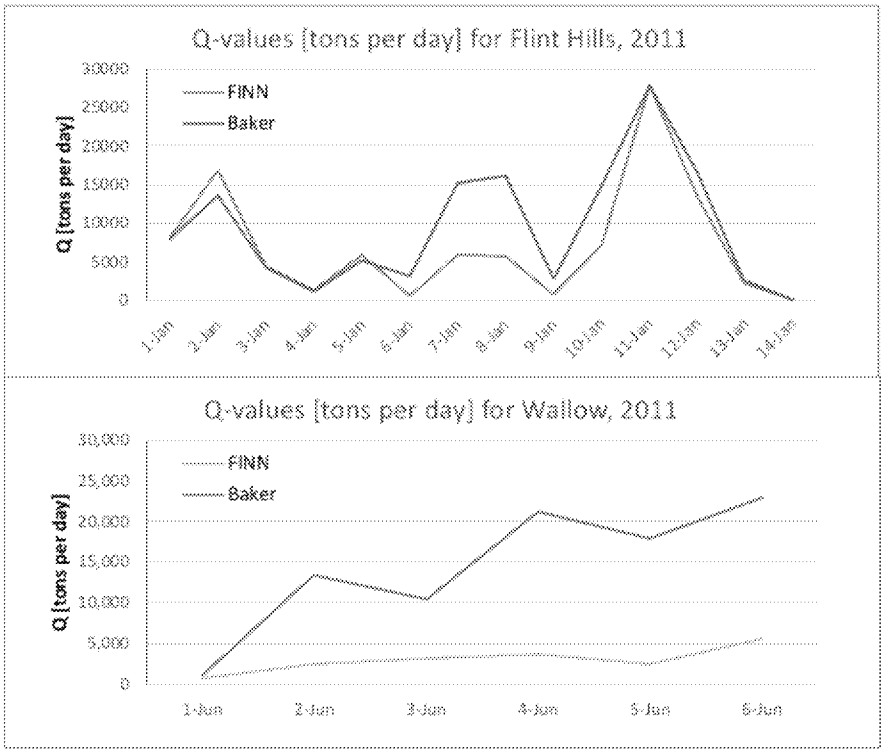

Figure 1. Emissions of VOC + NOx (Q) in tons per day for the Flint Hills and Wallow wildfire events from Baker et al. (2016) (blue) and from our estimate using the FINN database (orange).

Table 2: Summary of Q, D, and Ozone Enhancement Values from selected literature

Location	Q [tpd]	D [km]	Q/D [tpd/km]	O_3 Enhancement	Citation
Wallow	6,000	350	17.1	20	Baker et al. 2016
Flint Hills	28,000	250	112.0	25	Baker et al. 2016
Mexico City	14,000	150	93.3	0	Lei et al., 2013
Western Canada	80,000	1,500	53.3	10	Lindaas et al, 2017
Western US	34,000	1,350	25.2	10	Lindaas et al., 2017
Maryland	1,500	1,700	1.0	14	Dreessen et al., 2016
Western US	70,000	1,100	63.6	14	Gong et al. 2017
Western US	70,000	1,000	70.0	8	Gong et al. 2017
Western US	70,000	500	140.0	16	Gong et al. 2017
Western US	70,000	500	140.0	10	Gong et al. 2017
Western US	70,000	300	233.3	15	Gong et al. 2017
Western US	70,000	150	466.7	13	Gong et al. 2017
Alaska and Canada	100,000	4,000	25.0	50	Morris et al., 2006

NOTES: Alaska and Canada Q estimate very approximate, see Turquety et al. (2007)
Baker et al. (2016) D values are from fire centroids and nearest point in Texas

Figure 1 plots the Baker et al. (2016) estimates for the Q-values alongside our estimates for the same fire events using the FINN database. For the longer wildfire event (Flint Hills) our FINN estimate is similar to the Baker et al. (2016) estimate, except for the period between January 7 and 10, which we are up to a factor of 3 lower. Throughout the Wallow fire event, our FINN estimate is on average a factor of 5 lower than the Baker et al. (2016) estimate. Uncertainties in estimate Q-values are high, and include differences in the methodologies (the SmartFire/BlueSky methodology of Baker et al (2016) versus the FINN methodology used in our analysis). For the Wallow wildfire event, Baker et al. (2016) estimate much higher rVOC and NO_x than our methodology, possibly due to a FINN underestimation of emissions.

We also calculate Q-values for other fire events noted in the literature, summarized in Table 1, including 2013 fires in the Western US (Gong et al., 2017; Lindaas et al., 2017; Liu et al., 2017), the Fort McMurray wildfire in Canada in 2016 (Wentworth et al., 2018), a large wildfire event in Alaska and Canada (Morris et al., 2006), 2011 fires in Maryland (Dreessen et al., 2016), and, available estimates for the Yucatan Peninsula in Mexico (Yokelson et al., 2009), and the Flint Hills and Wallow wildfires from Baker et al. (2016). Excluding the largest fires (>70,000 tpd from Lindaas et al., 2017; Gong et al, 2017, and Morris et al., 2006), we find that a large fire was a Q-value of approximately 40,000 tpd. We use this large Q-value as a demonstration of the Q/D metric in Figure 2 for a typical large wildfire event, which plots the Q/D values for Q-values ranging from 100 – 40,000 tpd and D-values ranging from 1 – 1,000 kilometers.

Q/D	1000	750	500	400	300	200	150	100	75	50	25	20	15	10	5	2.5	1	km
40,000	40	53	80	100	133	200	267	400	533	800	1,600	2,000	2,667	4,000	8,000	16,000	40,000	
38,000	38	51	76	95	127	190	253	380	507	760	1,520	1,900	2,533	3,800	7,600	15,200	38,000	
36,000	36	48	72	90	120	180	240	360	480	720	1,440	1,800	2,400	3,600	7,200	14,400	36,000	
34,000	34	45	68	85	113	170	227	340	453	680	1,360	1,700	2,267	3,400	6,800	13,600	34,000	
32,000	32	43	64	80	107	160	213	320	427	640	1,280	1,600	2,133	3,200	6,400	12,800	32,000	
30,000	30	40	60	75	100	150	200	300	400	600	1,200	1,500	2,000	3,000	6,000	12,000	30,000	
28,000	28	37	56	70	93	140	187	280	373	560	1,120	1,400	1,867	2,800	5,600	11,200	28,000	
26,000	26	35	52	65	87	130	173	260	347	520	1,040	1,300	1,733	2,600	5,200	10,400	26,000	
24,000	24	32	48	60	80	120	160	240	320	480	960	1,200	1,600	2,400	4,800	9,600	24,000	
22,000	22	29	44	55	73	110	147	220	293	440	880	1,100	1,467	2,200	4,400	8,800	22,000	
20,000	20	27	40	50	67	100	133	200	267	400	800	1,000	1,333	2,000	4,000	8,000	20,000	
18,000	18	24	36	45	60	90	120	180	240	360	720	900	1,200	1,800	3,600	7,200	18,000	
16,000	16	21	32	40	53	80	107	160	213	320	640	800	1,067	1,600	3,200	6,400	16,000	
14,000	14	19	28	35	47	70	93	140	187	280	560	700	933	1,400	2,800	5,600	14,000	
12,000	12	16	24	30	40	60	80	120	160	240	480	600	800	1,200	2,400	4,800	12,000	
10,000	10	13	20	25	33	50	67	100	133	200	400	500	667	1,000	2,000	4,000	10,000	
9,000	9	12	18	23	30	45	60	90	120	180	360	450	600	900	1,800	3,600	9,000	
8,000	8	11	16	20	27	40	53	80	107	160	320	400	533	800	1,600	3,200	8,000	
7,000	7	9	14	18	23	35	47	70	93	140	280	350	467	700	1,400	2,800	7,000	
6,000	6	8	12	15	20	30	40	60	80	120	240	300	400	600	1,200	2,400	6,000	
5,000	5	7	10	13	17	25	33	50	67	100	200	250	333	500	1,000	2,000	5,000	
4,500	5	6	9	11	15	23	30	45	60	90	180	225	300	450	900	1,800	4,500	
4,000	4	5	8	10	13	20	27	40	53	80	160	200	267	400	800	1,600	4,000	
3,500	4	5	7	9	12	18	23	35	47	70	140	175	233	350	700	1,400	3,500	
3,000	3	4	6	8	10	15	20	30	40	60	120	150	200	300	600	1,200	3,000	
2,500	3	3	5	6	8	13	17	25	33	50	100	125	167	250	500	1,000	2,500	
2,000	2	3	4	5	7	10	13	20	27	40	80	100	133	200	400	800	2,000	
1,500	2	2	3	4	5	8	10	15	20	30	60	75	100	150	300	600	1,500	
1,000	1	1	2	3	3	5	7	10	13	20	40	50	67	100	200	400	1,000	
500	1	1	1	1	2	3	3	5	7	10	20	25	33	50	100	200	500	
400	0	1	1	1	1	2	3	4	5	8	16	20	27	40	80	160	400	
300	0	0	1	1	1	2	2	3	4	6	12	15	20	30	60	120	300	
200	0	0	0	1	1	1	1	2	3	4	8	10	13	20	40	80	200	
100	0	0	0	0	0	1	1	1	1	2	4	5	7	10	20	40	100	
tpd																		

Figure 2: Values for Q/D (in tpd/km) for emissions of various sizes (Q, rows) and at various distances (D, columns). Blue values indicate Q/D is less than the 100 tpd/km threshold that differentiates Tier 2 and Tier 3 evidence, while white and warm colors indicate Q/D values above the 100 tpd/km threshold.

Figure 2 demonstrates that the Q/D metric will not identify significant wildfire events (i.e. Q/D > 100 tpd/km) if they are: (1) more than 400 km away, even if they are large events (up to 40,000 tpd); (2) small events (< 1000 tpd), even if they are nearby the receptors (~ 10 km); and (3) moderate events (~ 10,000 tpd) that are at an intermediate distance from the receptor (~ 100 km). There are many cases in which ozone enhancement is noted much farther than 400 km from a wildfire emissions source (e.g. Baker et al., 2016), as well as many cases in which little-to-no ozone enhancement is noted less than 400 km from the wildfire source (e.g. Lei et al., 2013; Wentworth et al., 2018).

We further explore the Q/D metric by highlighting case studies identified from the literature. Table 2 above and Figure 3 below show a collection of Q-values (either from the literature or, if Q-values are not in the literature, from our FINN estimation method described above) for wildfire events that could potentially impact Texas. If multiple days or events are listed in the literature, we chose the highest values. The distances (D) are estimates based on the approximate centroid for each wildfire emission source and the receptors as described in each

publication. Q/D values are then computed, and ozone enhancement values are listed when available in the cited publications. Figure 3 also includes estimates from adapted from Figure A2-1 in the EPA Exceptional Events Guidance Memo. We now briefly describe the general results as plotted in Figure 3, and then some of the details of the individual regions included.

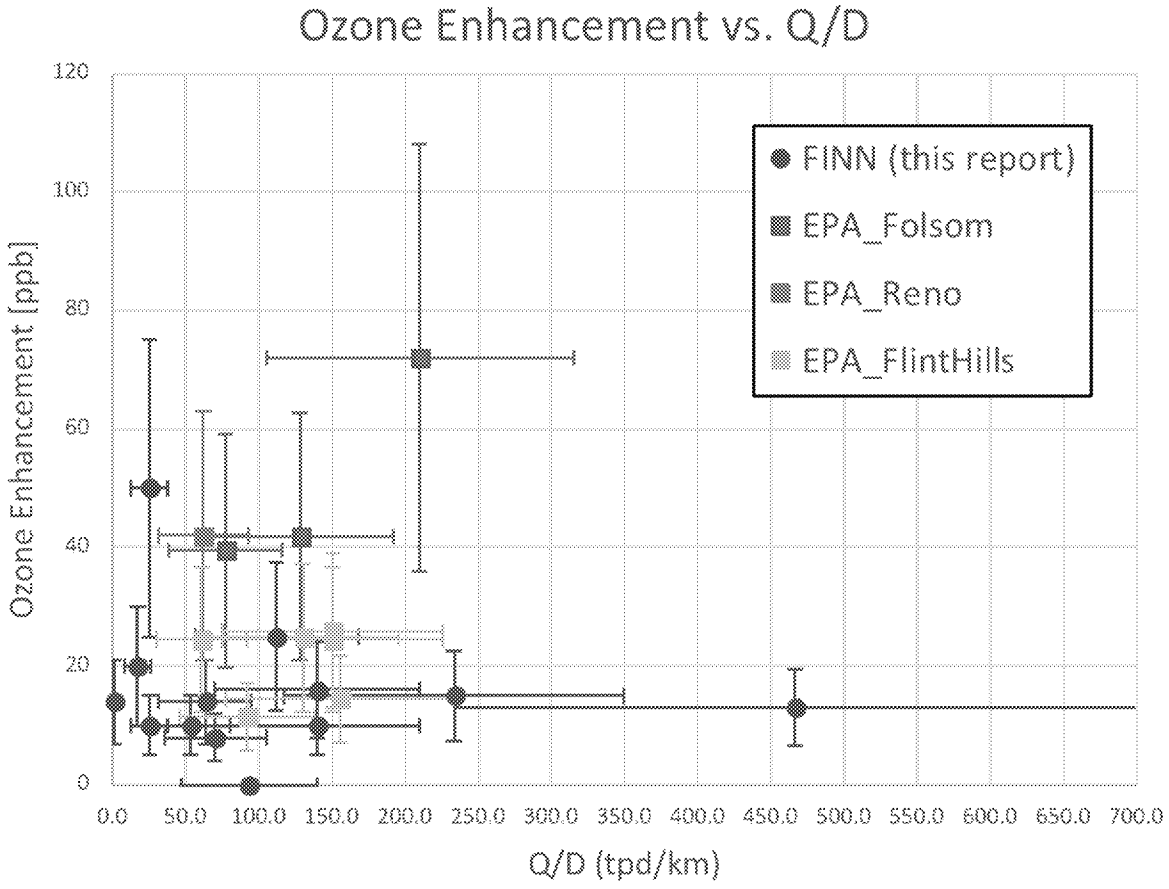

Figure 3: Comparison of Ozone Enhancement [ppbv] and Q/D Estimates [tpd/km] from this work (FINN, red) and from the EPA Guidance Memo (blue, grey, and yellow, adapted from Figure A2-1). All error bars are ± 50%.

Overall, the range and uncertainty in Q/D and ozone enhancement estimates are high (the error bars represent ±50% in Figure 3, based on the usual mean differences between fire emission inventories [Wiedinmyer et al., 2011]), with Q/D values ranging from 0 – 500 tpd/km and ozone enhancement values ranging from 0 – 80 ppbv. Below the 100 tpd/km threshold used to distinguish Tier 2 and Tier 3 demonstrations, estimates of the ozone enhancement values are almost uniformly distributed, with a slight tendency towards lower values (0 – 25 ppbv). The Folsom 2008 event from the EPA Guidance Memo is the clearest demonstration of a positive correlation between the Q/D metric and high ozone enhancement values, but when the data from all fires is included there is little correlation between ozone enhancement and the Q/D metric ($R^2 < 0.01$).

The Q/D metric can also miss significant ozone enhancements reported for distant fires. For example, Morris et al. (2006) describe a large wildfire event in Alaska, which significantly impacted ozone values in Texas (50 ppbv). The Q-value estimated here is a rough estimate, taking a maximum emission rate of 1 Tg CO per day and assuming VOCs and NO_x are roughly 10% of the CO emissions (Levine, 2014), but demonstrates that the Q/D metric is not capable of capturing very large wildfires originating from distance sources. There are very few studies examining wildfire emissions from the Yucatan Peninsula in Mexico (Cofer et al, 1993; Yokelson et al., 2009). Both made aircraft measurements, and while wildfire plumes do occasionally reach Texas (as demonstrated by forward trajectories from Yokelson et al., 2009) there are no estimates of the potential ozone enhancement. The other sources included in Figure 3 and Table 1 are from other US states, primarily from the Western US (Gong et al., 2016; Lindaas et al., 2017; Liu et al., 2017).

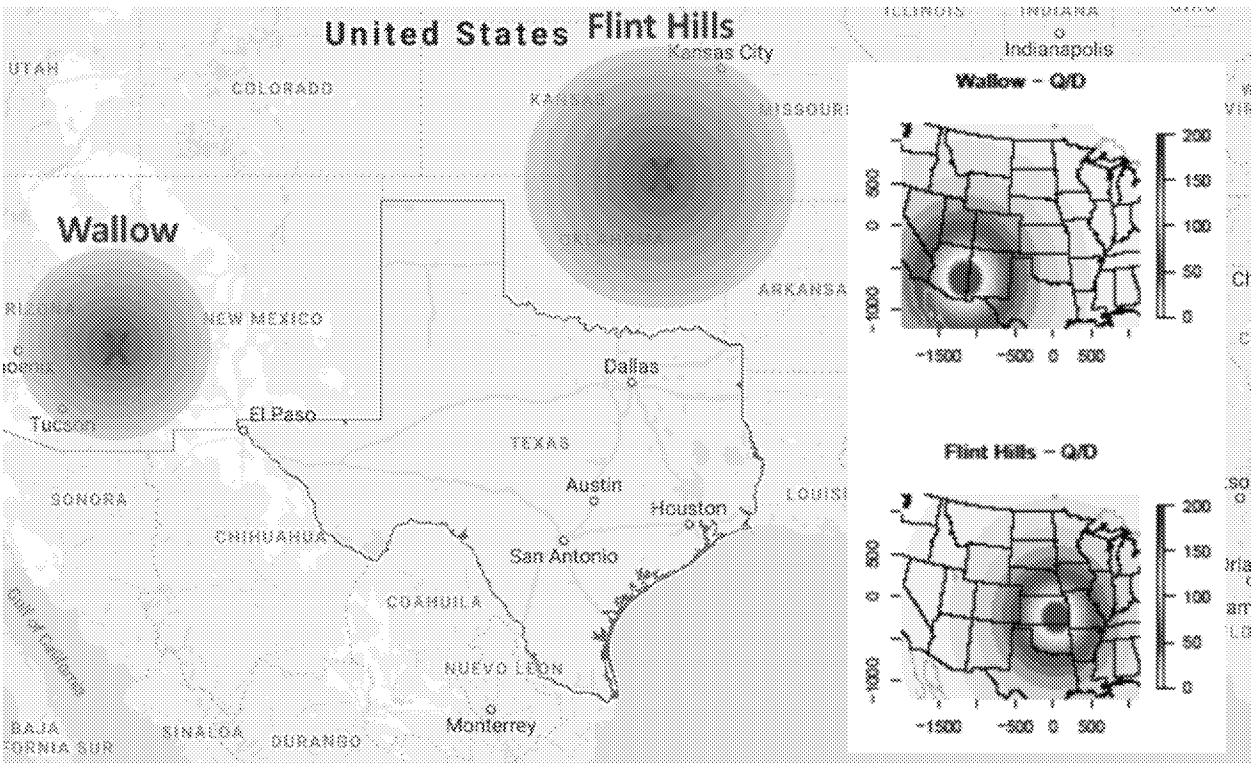

Figure 4: Q/D values in excess of 100 tpd/km for the Wallow and Flint Hills 2011 fires. Insert is the Q/D analysis from Baker et al. (2016). The analysis of Craig et al. (2013) supports these results.

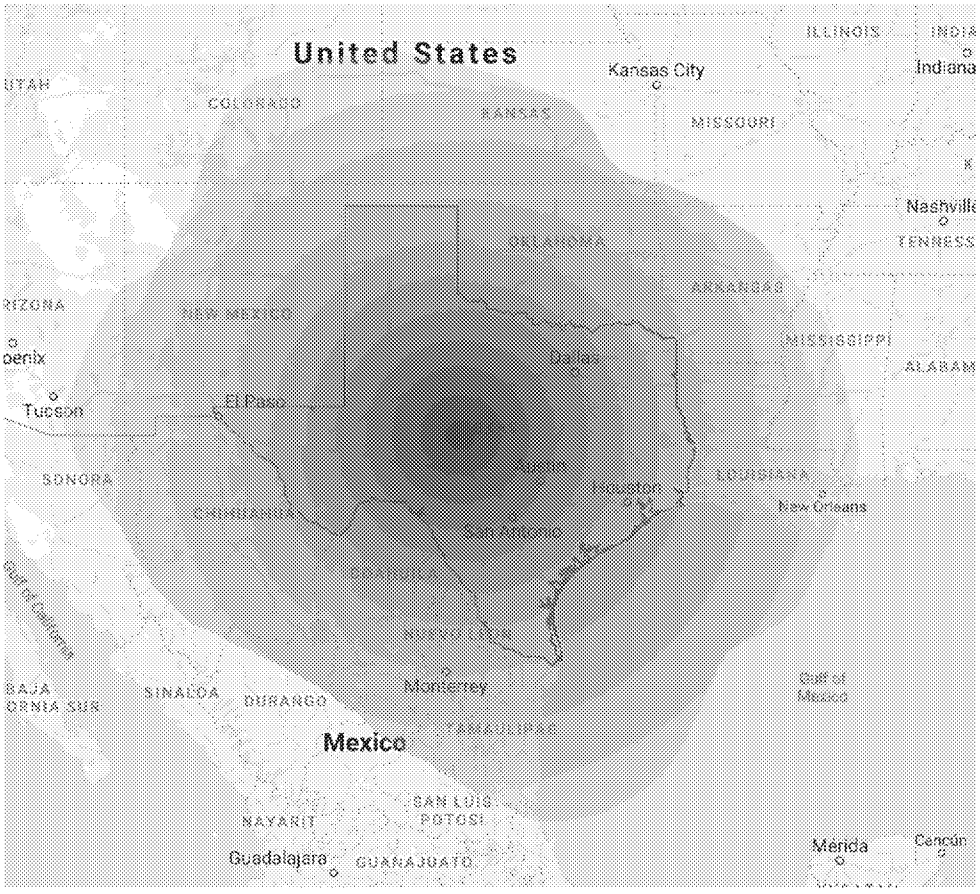

Figure 5: Approximately 400 km range extended out from the Texas state border, roughly the distance (D) a 40,000 tpd (Q) fire event would need to be if it were to exceed the Q/D = 100 tpd/km threshold for a receptor within the Texas state border.

The Q/D metric also appears to screen out several fires close to Texas that reported significant ozone impacts. For example, Baker et al. (2016) present estimates for two fires, Wallow and Flint Hills, for different days and so are compared to our estimates (above). These fires are relatively close to Texas (originating in nearby states), although their Q/D values do not exceed the 100 tpd/km values anywhere within Texas (see Figure 4).

Figure 5 plots the 400-kilometer footprint surrounding the state of Texas, which shows that it is unlikely for a large fire, even one as large as the Fort McMurray fire, to be close enough to Texas to exceed the 100 tpd/km threshold. Figure 4 plots the regions which exceed the 100 tpd/km threshold for the Wallow and Flint Hills wildfires documented in Baker et al. (2016), neither of which lie over any air basin within Texas.

For Texas, this implies that in order to qualify as capable of Tier 2 analysis, assuming an approximate 1-in-10-year fire event, the event would have to occur within the indicated regions in Figure 5 above This is not a large region, and there are many cases of documented cases of wildfire influence on ozone in Texas from wildfires well outside of this region (Jaffe and Wigder, 2012; Jaffe et al., 2013 and references therein). Thus, unless a large wildfire event occurred between the Texas border and Albuquerque, Denver, Tulsa, Memphis, New Orleans, Tampico, and Parral, Mexico, Texas would have to gather Tier 3 level evidence following the EPA Guidance Memo.

This excludes fires from the Yucatan, from most of Colorado, most of Mexico, and almost the entire Western and Central US.

Smaller events would have to be proportionally closer to the Texas state border to qualify for Tier 2 level analysis, and even the Wallow and Flint Hill fire events of 2011 (Baker et al., 2016) do not achieve, or are borderline cases, for the Tier 2 level evidence, even though there is clear evidence that these fire events impacted ozone levels within the Texas state borders (see Baker et al., 2016). This implies that Texas will rarely qualify for Tier 2 level exceptional event classification for any but the clearest exceptional event cases.

2.3 Evaluation of the Q/D Metric

As reviewed in the previous section, wildfire plumes that advect into air basins have the potential trigger ozone enhancement events, but the complex interactions of chemistry and meteorology do not allow for confidence that the presence of a wildfire plume itself will guarantee significant ozone enhancement. Ozone enhancement can occur nearby (e.g. Junquera et al., 2005) and far from wildfires (e.g. McKeen et al., 2002; Morris et al., 2006; Real et al., 2007), but there are also many cases where no ozone enhancement is noted nearby wildfires (e.g. Wentworth et al., 2018; Lei et al., 2013). Estimates of ozone enhancement due to wildfire impact can range from relatively modest increases of ~ 10 ppbv (e.g. Pfister et al., 2008) and reach up to 30 – 60 ppbv (e.g. Junquera et al., 2005; Morris et al., 2006; Singh et al., 2012; Brey and Fischer, 2016; Baker et al., 2016), although there are also many cases where little-to-no ozone enhancement is noted (e.g. Tanimoto et al., 2008; Verma et al., 2009; Alvarado et al., 2010; Singh et al., 2012; Zhang et al., 2014; Lu et al., 2016; Bytnerowicz et al., 2016; Lindaas et al., 2017), and even some cases where the presence of wildfire plumes decrease ozone concentrations (e.g. vanCuren and Gustin, 2015).

A canonical wildfire-induced ozone enhancement event, generally meets the following criteria: (1) high VOC concentrations, typically within the wildfire plume; (2) high NO_x concentrations, either originating from wildfire emissions themselves, PAN decomposition within the wildfire plume, or from non-plume sources (e.g. anthropogenic emissions, see Akagi et al., 2013); (3) sufficient solar radiation to induce the photolysis reactions necessary for rapid O_3 production; and (4) meteorological conditions conducive to O_3 production, such as high temperatures, low winds (Jacob and Winner, 2009), and low humidity (Lu et al., 2016).

If one or more of these criteria are not met – and even sometimes when all the criteria are met (e.g. Lei et al., 2013; Wentworth et al., 2018) – wildfire plumes may not trigger any significant ozone enhancement, or even may trigger ozone suppression. For example, the 2016 Fort McMurray / Horse River Wildfire in Alberta, Canada is a recent, extreme wildfire event that burned over 500,000 hectares (Landis et al., 2018; Wentworth et al., 2018). There were multiple air quality monitoring sources located in and around the wildfire burn zone (Wentworth et al., 2018), although negligible ozone enhancement was noted (Wentworth et al., 2018). Some monitors registered exceptionally high ozone mixing ratios (1500 – 7000 ppbv), although these appear to be instrumental artifacts (Landis et al., 2018). Downwind impacts of this fire have not been reported in the literature, although they may be forthcoming.

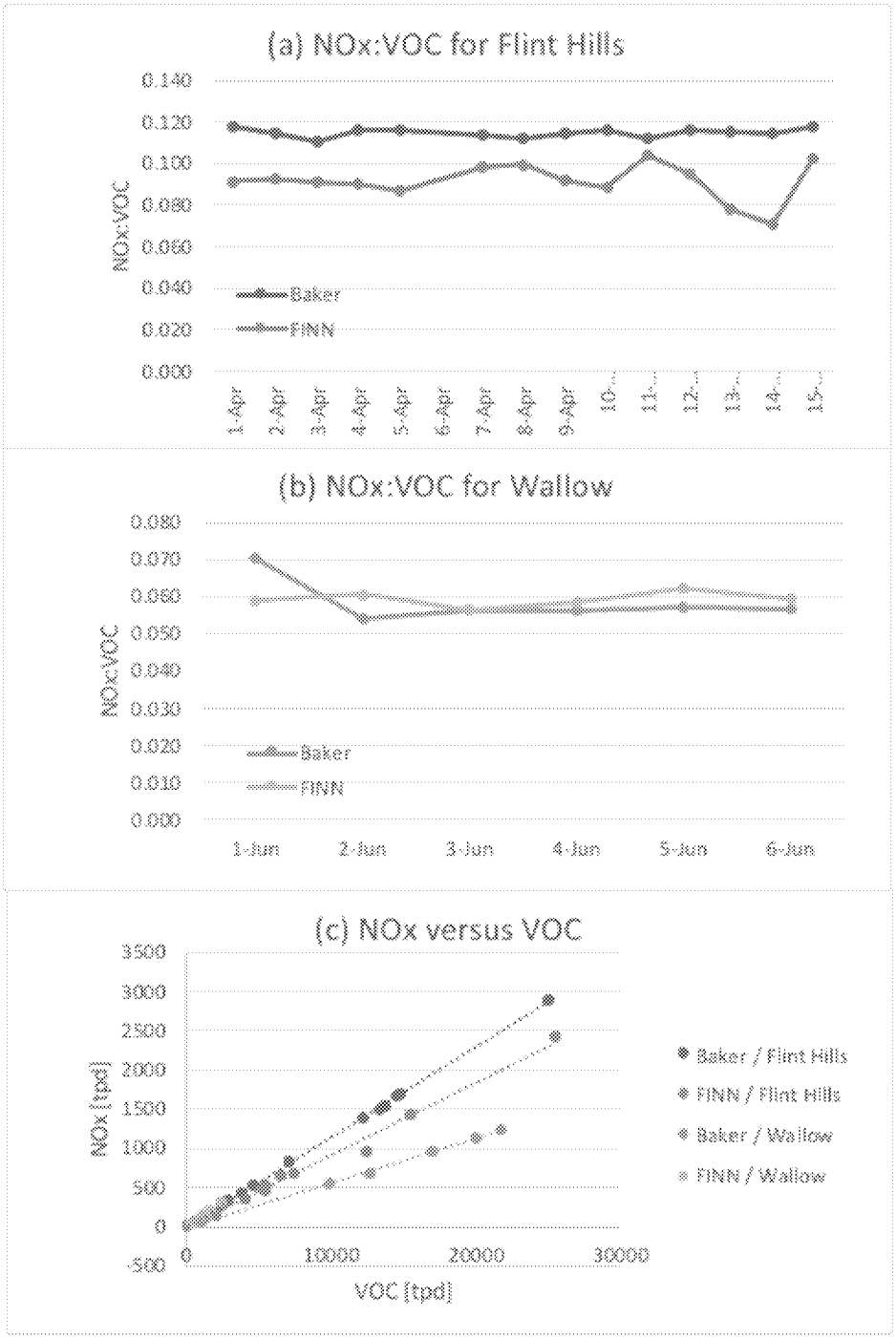

Figure 6: NO_x:VOC ratios time series for (a) Flint Hills and (b) Wallow and (c) NO_x versus VOC plots.

Consequently, a metric such as the EPA's Q/D metric, which inherently assumes a linear relationship between rVOC, NOx, distance, and ozone, is useful only as an indication of the proximity of a receptor to a wildfire of a given magnitude. It can indicate at most the *potential* for

wildfire influence on ozone formation but cannot be used as sufficient evidence (which the EPA Guidance Memo acknowledges).

Furthermore, as we show in Figures 4 and 5, the Q/D metric is not a particularly helpful metric for determining the likelihood that a nearby and upwind wildfire may or may not impact Texas air quality. The Wallow and Flint Hill fires described in Baker et al. (2016) impacted Texas air quality, but an assessment of the Q/D metric for these fires would not have indicated this to be the case. Only for a small set of wildfires would the Q/D metric trigger a Tier 2 level of evidence and demonstration, and as such this metric is not of great value in Texas. The other metrics used to demonstrate an exceptional event due to wildfires (such as the back-trajectories, time-series of the receptors, etc.) are far more efficient at demonstrating the influence of wildfires on air quality within Texas.

Since the Q-metric is defined as the sum of rVOCs and NO_x, we also include in Figure 6 the VOC:NO_x ratio as estimated through our analysis of the FINN data and from Baker et al. (2016). Generally, NO_x make up 5 – 20% of the Q-values. The different estimation methods between the Baker et al. (2016) study and our FINN analysis are evident, in that we estimate a roughly 30% lower NO_x:VOC ratio than the Baker et al. (2016) estimates, although the estimates of NO_x:VOC ratios vary from fire-to-fire. The NO_x versus VOC plot (Figure 6c) shows that for both the Flint Hills and Wallow fires, each estimation method (Baker et al., 2016 and our FINN analysis) have a consistent NO_x:VOC ratio, demonstrated by the linear nature of NO_x:VOC in Figure 6c. High NO_x concentrations within wildfire plumes are likely to enhance ozone formation, so improved estimates of the proportion of NO_x within estimates of the Q-values may provide another avenue for the identification of potential wildfire influenced ozone enhancement events.

3 Assessing Q/D During Biomass Burning Events Impacting HGB

In this task we used the ASP (Section 3.1) and STILT-ASP (Section 3.2) models to simulate the O_3 formation in biomass burning plumes in two events when fires in the Yucatan impacted the Houston/Galveston/Brazoria (HGB) urban areas, as identified in previous work by Prof. Yuxuan Wang of the University of Houston. The two events simulated will be April 26-27, 2011 and May 1-2, 2013. In both of these events, the maximum MDA8 O_3 in HGB exceeded 70 ppbv, making them good surrogates for the types of events likely to be included in exceptional event demonstrations in the future.

3.1 ASP Simulations

We used ASP v2.1.1 in this work, which differs from ASP v2.1 (Alvarado et al., 2015) only in that it includes minor bug fixes and additional features for the simulation of smog chamber experiments. These simulations all used ASP in a Lagrangian parcel model that is assumed to be well-mixed in the boundary layer and expanding horizontally with time as background air is mixed in (Alvarado et al., 2009, 2015). The model was set to use the chemical mechanism described in Alvarado et al. (2015), and as in that study we assumed that deposition had a negligible impact on the parcel-mean gas-phase concentrations of different species over the two-day period simulated here. Emission factors for four different fuel types/biomes (Tropical Forest, Temperature Forest, Boreal Forest, and Savannah/Grassland) were taken from the reviews of Akagi et al. (2011) and Andreae and Merlet (2001) following the approach used in Alvarado et al. (2015). However, as this work focuses on the O_3 impacts of the fires and not the fire impacts on $PM_{2.5}$, we did not include any semi-volatile or intermediate volatility compounds in the fire emissions and we ran ASP with the aerosol condensation and coagulation routines turned off. However, to prevent this from resulting in an unphysical overestimate of the fraction HNO_3 back to NO_x, the reaction of HNO_3 with OH was deactivated in these simulations. This accounts for the fact that the HNO_3 produced in the NH_3-rich environment of a biomass burning plume generally quickly partitions to the aerosol phase and is not available for such chemistry. Cloud-free photolysis rates were calculated using TUV v5.0 (Madronich and Flocke, 1999) for May 1, 2013 and the latitude of the Tropic of Cancer (23.44 ^{o}N), which lies between the Yucatan and the HGB urban area. The assumption of cloud-free skies and no deposition will tend to result in overestimates of the O_3 formation rate in our simulations. However, our goal here is to study how this formation varies with distance, not to get the exact amount formed, and the STILT-ASP simulations in Section 3.2 account for both clouds and deposition of O_3 and other gases.

The initial width of the plume was set to 200 km as that is approximately the square root of the area of the Yucatan (39524 km^2). The horizontal eddy diffusion coefficient for a plume this size is around 10^4 m^2/s (Gifford, 1981), which gives an initial plume mixing timescale of 10^6 s, or about 11.6 days. For this slow mixing timescale, background concentrations do not have a significant impact on the plume chemistry, but note that we are not able to account for large-scale stretching and mixing of the plume by synoptic-scale motions in this simplified parcel model. For these simulations, the background concentration for NO_x was set to 0.06 ppbv, the background concentration of O_3 to 50 ppbv, and the background concentration of CO to 100 ppbv. Background concentrations for VOC species were set to 0.

ASP v2.1.1 can be run with a fixed set of emission factors, with the initial plume concentrations for all species calculated based on the initial CO concentration and these emission factors (including the initial titration of background O_3 by the NO emissions). Our goal was to

estimate a reasonable value for this initial plume-average concentration given the conditions of the Yucatan during the fire events studied here, not to attempt to get a precise estimate for each day. We estimated a high value for the initial CO concentration using the FINN estimates of the CO emissions from the Yucatan on April 26, 2011 (156,000 tons per day), an assumed temperature of 295 K, an assumed pressure of 950 ppbv, a boundary layer height of 2 km, a relative humidity of 70%, and that the parcel accumulated 8% of the days fire emissions passing over the Yucatan. This resulted in an estimate of 150 ppbv CO added to the parcel from the Yucatan fires (ΔCO_{init} = 150 ppbv), for a total initial CO concentration of 250 ppbv. As our assumed values above are highly uncertain, we also tested two other values of the CO added by the fire: 225 ppbv and 75 ppbv (Section 3.1.2).

3.1.1 Baseline Results

As the Yucatan is primarily covered by tropical forest, we chose the conditions for our baseline simulation to be ΔCO_{init} = 150 ppbv with tropical forest emission factors and the parcel being emitted from the Yucatan fires at noon. We assumed a two-day travel timescale between the Yucatan and the HGB urban area based on the STILT-ASP back-trajectories for these events.

Figure 7 shows the impact of the fire emissions on CO (left) and O_3 (right) in the parcel over the 48 hours simulated, calculated as the difference between the in-plume concentration and the assumed constant background concentrations of 100 ppbv CO and 50 ppbv O_3. As this parcel is starting at local noon time, there is a rapid initial production of O_3 in the plume leading to an enhancement of ~30 ppbv (total O_3 of ~80 ppbv) by the first night of the simulations. There is also an initial burst of secondary CO production as the fire VOCs are oxidized, but then the CO gradually decreases in line with the large mixing timescale of this large plume. Both of these behaviors are consistent with the expected behavior of large biomass burning plumes (e.g., Akagi et al., 2012). As the fire NO_x has been depleted by the second day (from 5 ppbv to 0.4 ppbv), the O_3 production on the second day is smaller (~10 ppbv), leading to an estimated fire O_3 impact of ~40 ppbv after 48 hours. Note that this shows that, for the same level of emissions, the impact of the fires on O_3 can be much larger further downwind from the fire than it is close to the fire, which is not consistent with the Q/D metric.

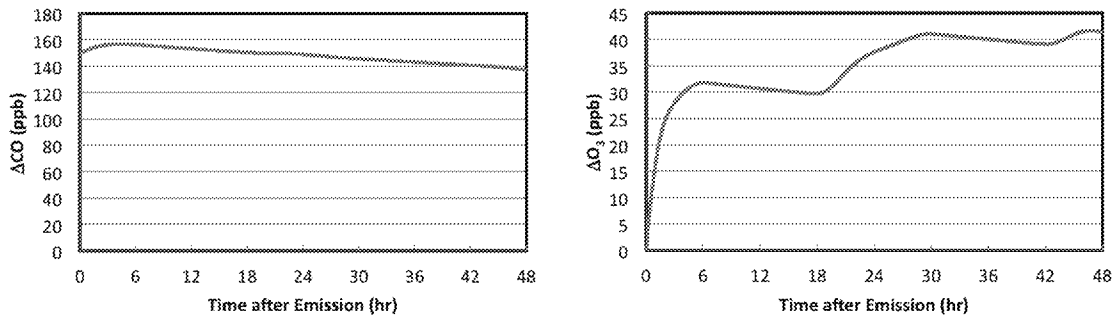

Figure 7. Fire enhancement of CO (left) and O_3 (right) versus time after emission for the baseline simulation.

To further examine if this O_3 formation is consistent with the Q/D metric, we plotted the CO and O_3 enhancements as a function of the reciprocal of the plume age (Figure 8). If the wind

speed and direction is constant, this is the same as plotting the data as a function of 1/D, and as the Q is constant for this case by definition, it approximates a Q/D plot. We can see that the CO enhancement is consistent with the Q/D metric, as it makes a fairly flat line when plotted this way before sharply decreasing at large distances (low values of Q/D). However, the impact of the fires on O_3 is *not* constant as a function of Q/D – instead, O_3 shows a significant increase for high values of D (low values of Q/D). In fact, the only time the O_3 impact decreases as Q/D decreases is at night. Thus the non-linear formation of O_3 in biomass burning plumes is not well represented by the Q/D screening metric.

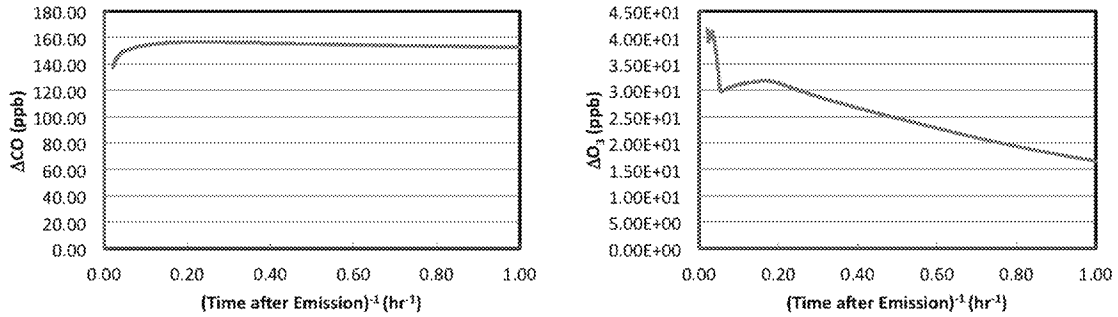

Figure 8. Fire enhancement of CO (left) and O_3 (right) versus the reciprocal of time after emission for the baseline simulation.

3.1.2 Sensitivity to Emissions and PBL Heights

In the Lagrangian parcel framework we are using here, the sensitivity of the results to daily changes in fire emissions, errors in the PBL height, and errors in the diurnal dependence of the emissions are all incorporated via the initial CO enhancement (ΔCO_{init}). Figure 9 shows how the O_3 formation in the plume changes with different values of ΔCO_{init} between 75 to 225 ppbv. After the first few hours we can see the O_3 formation is roughly proportional to the change in the initial concentration of CO (and thus the fire emissions of NO_x and VOCs, or the change in the PBL height, etc.).

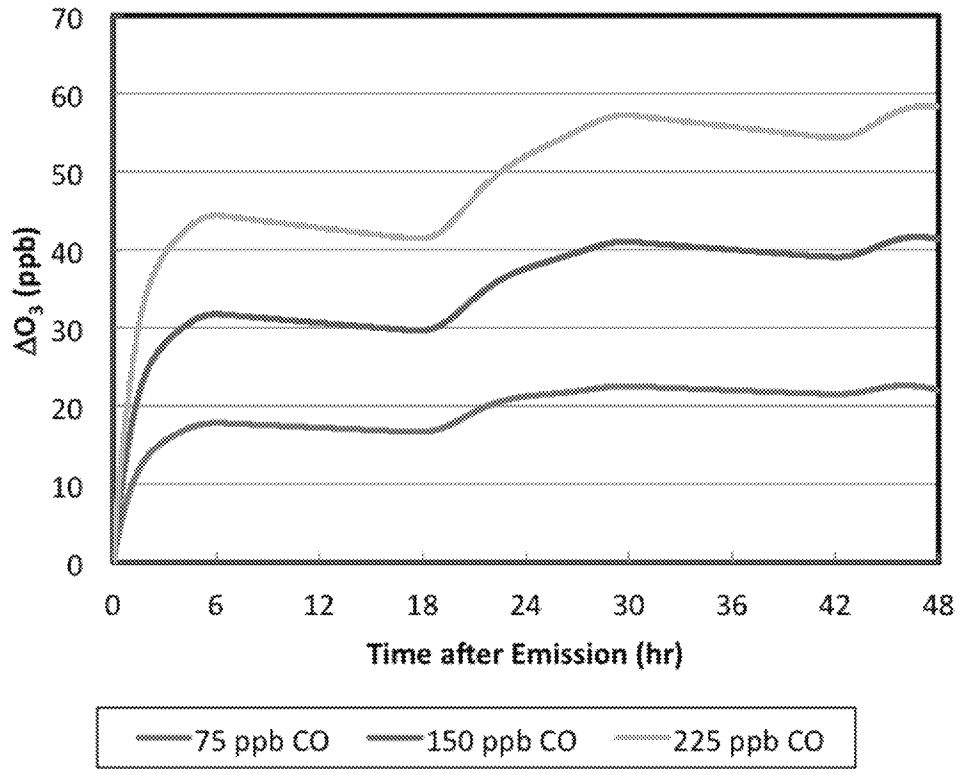

Figure 9. Fire enhancement of O_3 versus time after emission for different values of ΔCO_{init}. All simulations use the tropical forest emission factors with the parcel being emitted from the Yucatan fires at noon as in the baseline simulation.

However, translating these results in terms of Q/D requires an assumption about whether the change in ΔCO_{init} is caused by a change in fire emissions or a change in other parameters needed to calculate ΔCO_{init} like the PBL height or fire area. If the change in ΔCO_{init} is due to difference in fire emissions only, then the fire O_3 enhancement does scale roughly linearly with emissions. However, if the difference in ΔCO_{init} is due to changes in the boundary layer height or fire area, with the emissions held constant, then we would get very different values for the O_3 impact for the fires for the same value of Q/D. This suggests the Q/D metric is insufficient to assess the potential O_3 impact of the fires without incorporating this additional information.

3.1.3 Sensitivity to Fire Fuel Type

An implicit assumption of the Q/D metric is that all fires have similar changes in O_3 with distance, and that any variation can be accounted for by scaling this dependence by the sum of the NO_x and VOC emissions from the fire (the "Q"). However, O_3 formation in fires is generally NO_x limited (e.g., Alvarado et al., 2009) and the NO_x to VOC ratio in the fire emissions changes dramatically between relatively high values for grassland fires and relatively low values for boreal forest fires. Thus the amount of O_3 formed for similar fire sizes (measured in terms of the total CO emission) can be very different for fires in these different fuel types. Figure 10 illustrates this by comparing the O_3 formation in the baseline simulation with similar simulations where the emissions factors for temperate forests, boreal forests, and grasslands are used, all starting with

ΔCO_{init} = 150 ppbv. As expected from their NO_x to VOC ratios, the highest O_3 impact is from the grassland fire (~50 ppbv after two days), with a much lower O_3 formation from the boreal fire (~10 ppbv after two days). However, this is not what one would expect if you used the sum of the NO_x and VOC emission factors in each fire as your guide. This sum is 40.2 g/kg burned for boreal forest fires, but is only 24.7 g/kg burned for grasslands. Thus, the Q/D metric, where Q is the sum of the NO_x and VOC emissions, implies an opposite dependence of O_3 with fuel type than that given in the ASP simulations.

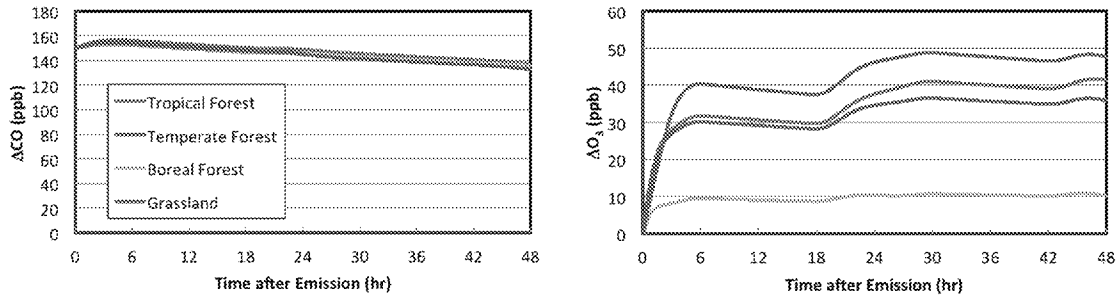

Figure 10. Fire enhancement of CO (left) and O_3 (right) versus time after emission for four different fuel types. All simulations have ΔCO_{init} = 150 ppbv with the parcel being emitted from the Yucatan fires at noon as in the baseline simulation.

To further investigate this issue, we derived a "Q/T" metric for each of the simulations in Figure 10, where the "Q" is the sum of the NO_x and VOC emission factors and the "T" is the time after emission, which is proportional to distance if the wind speed and direction is constant. The dependence of the O_3 enhancement on this metric for each case is shown in Figure 11. We can see that the dependence is fairly similar (i.e., within a factor of 2) for the tropical forest, temperate forest, and grassland fires. However, boreal forest fires are clearly different, with much lower O_3 formation. Thus a screening threshold for the Q/D metric that is appropriate for non-boreal fires will dramatically overestimate the O_3 impact from boreal fires.

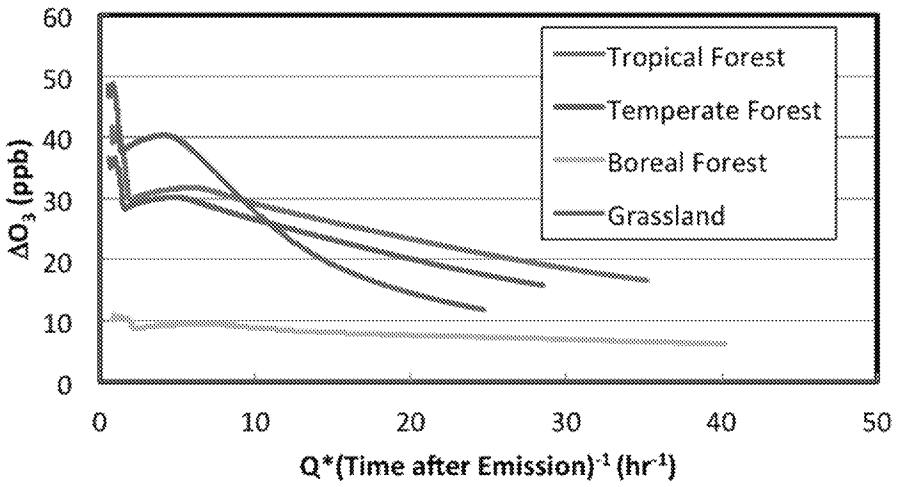

Figure 11. Fire enhancement of O_3 (right) versus the "Q/T" metric described in the text, where Q is the sum of the NO_x, HONO, and VOC emission factors and T is the time after emission. All simulations have ΔCO_{init} = 150 ppbv with the parcel being emitted from the Yucatan fires at noon as in the baseline simulation.

3.1.4 Sensitivity to Parcel Emission Time

A further complication for the Q/D metric could be due to the fact that the rate of O_3 formation in biomass burning plumes depends significantly on the photolysis rates, and thus the total O_3 formed in the plume at a given distance may depend on the time of day that the initial parcel was emitted. We tested this by changing the emission time for the baseline simulation in Section 3.1.1 and examining the differences in O_3 formation (Figure 12). While the dependence of the O_3 enhancement with emission time is fairly significant in the first day after emission, we can see that after two days all the simulations have settled down to similar O_3 enhancements (32-42 ppbv).

The consequences of this for the Q/D metric are shown in Figure 13, where the O_3 enhancements are plotted as a function of the reciprocal of the emission time, as in Section 3.1.1. We can see that the O_3 impact is extremely different for x-axis values of 0.2 hr^{-1} or higher, as the O_3 impact can vary between 0 ppbv to 30 ppbv depending on the time after emission.

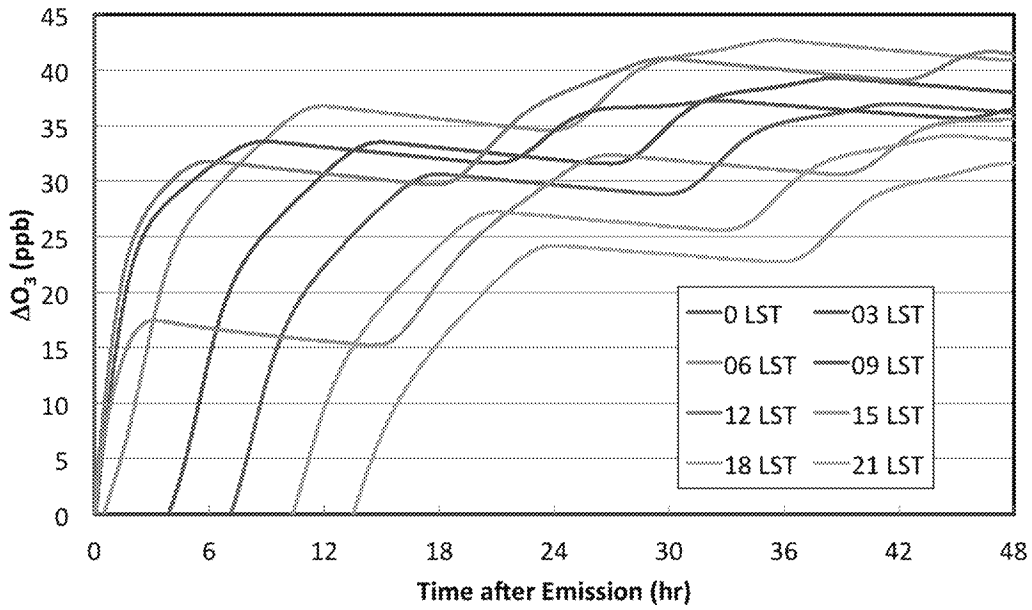

Figure 12. Fire enhancement of O_3 versus time after emission for different initial emission times. All simulations have ΔCO_{init} = 150 ppbv and tropical forest emission factors as in the baseline simulation.

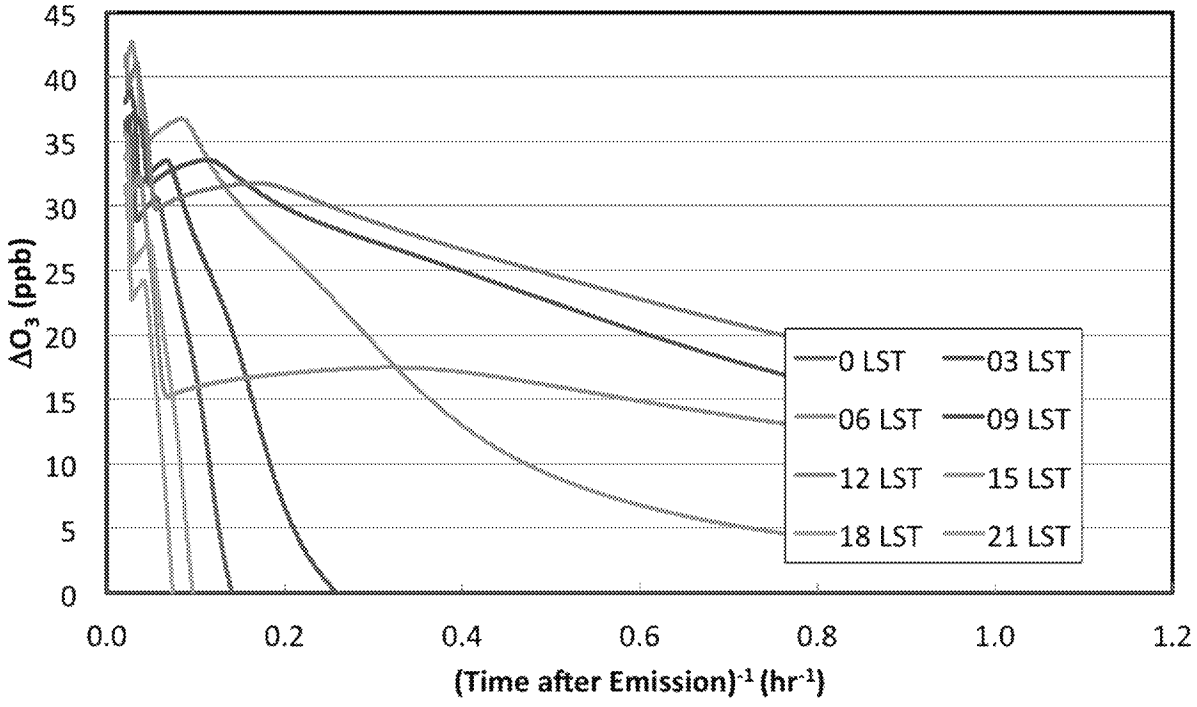

Figure 13. Fire enhancement of O_3 versus the reciprocal of time for different initial emission times. All simulations have ΔCO_{init} = 150 ppbv and tropical forest emission factors as in the baseline simulation.

3.2 STILT-ASP Simulations

We used STILT-ASP v2.1 in this work, which includes corrections to the biogenic emissions from those in STILT-ASP v2.0 (Alvarado et al., 2017). STILT-ASP v2.1 combines the Lagrangian particle dispersion model STILT (Lin et al., 2003) with ASP v2.1.1 to develop a Lagrangian chemical transport model. In STILT-ASP v2.1, back-trajectories are calculated using the 32-km horizontal meteorology from the North American Regional Reanalysis (Mesinger et al., 2006), the fire emissions come from the FINN inventory (Wiedinmyer et al., 2011, speciated to follow the ASP v2.1.1 chemical mechanism), the anthropogenic emissions come from the TCEQ 2012 modeling platform, and the biogenic emissions are calculated using the MEGAN v2.10 model (Guenther et al., 2006). Based on recent evaluations of STILT-ASP to determine the optimal configuration for the model (Alvarado et al., in prep.), STILT-ASP was run using 500 parcels for five-day back-trajectories, except for May 1, 2013 where some parcels left the NARR domain within 96 hours. In addition, early analysis of the calculated back-trajectories for April 27, 2011 showed that the maximum hourly O_3 in HGB for this date had little influence from fire emissions in the Yucatan (Figure 17). Thus, the rest of our analysis focuses on three dates: April 26, 2011; May 1, 2013, and May 2, 2013.

However, before we explore the STILT-ASP simulations for these three dates, we have selected three back-trajectories form the May 1, 2013 case so that we can explore the complex interactions between ozone wildfire enhancements and the Q/D metric. We selected these three back-trajectories as they all pass over the Yucatan Peninsula, but they each have unique characteristics that complicate the interpretation of the Q/D metric: the first back-trajectory does not follow a straight path from the Yucatan to the receptor and demonstrates complex ozone chemistry; the second back-trajectory originates to the east of the Yucatan Peninsula and advects over it, but shows little ozone enhancement; the third particle originates within the Yucatan Peninsula and follows a mostly straight path from the Yucatan to the receptor and demonstrates highly variable ozone chemistry. These back-trajectories are plotted in Figure 14.

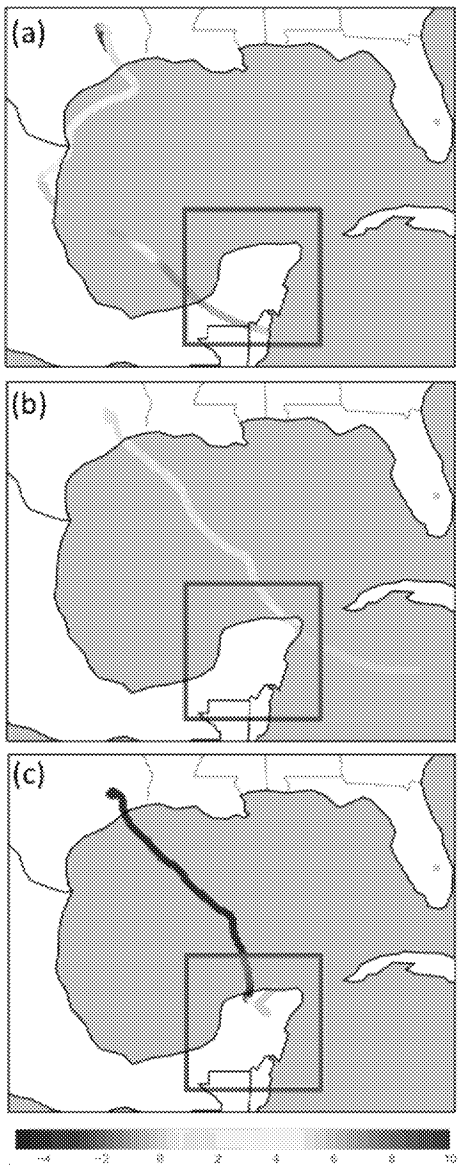

Figure 14: Three parcels from the May 1, 2013 case. The red box is the Yucatan region, and the color of the trajectories is the wildfire ozone enhancement.

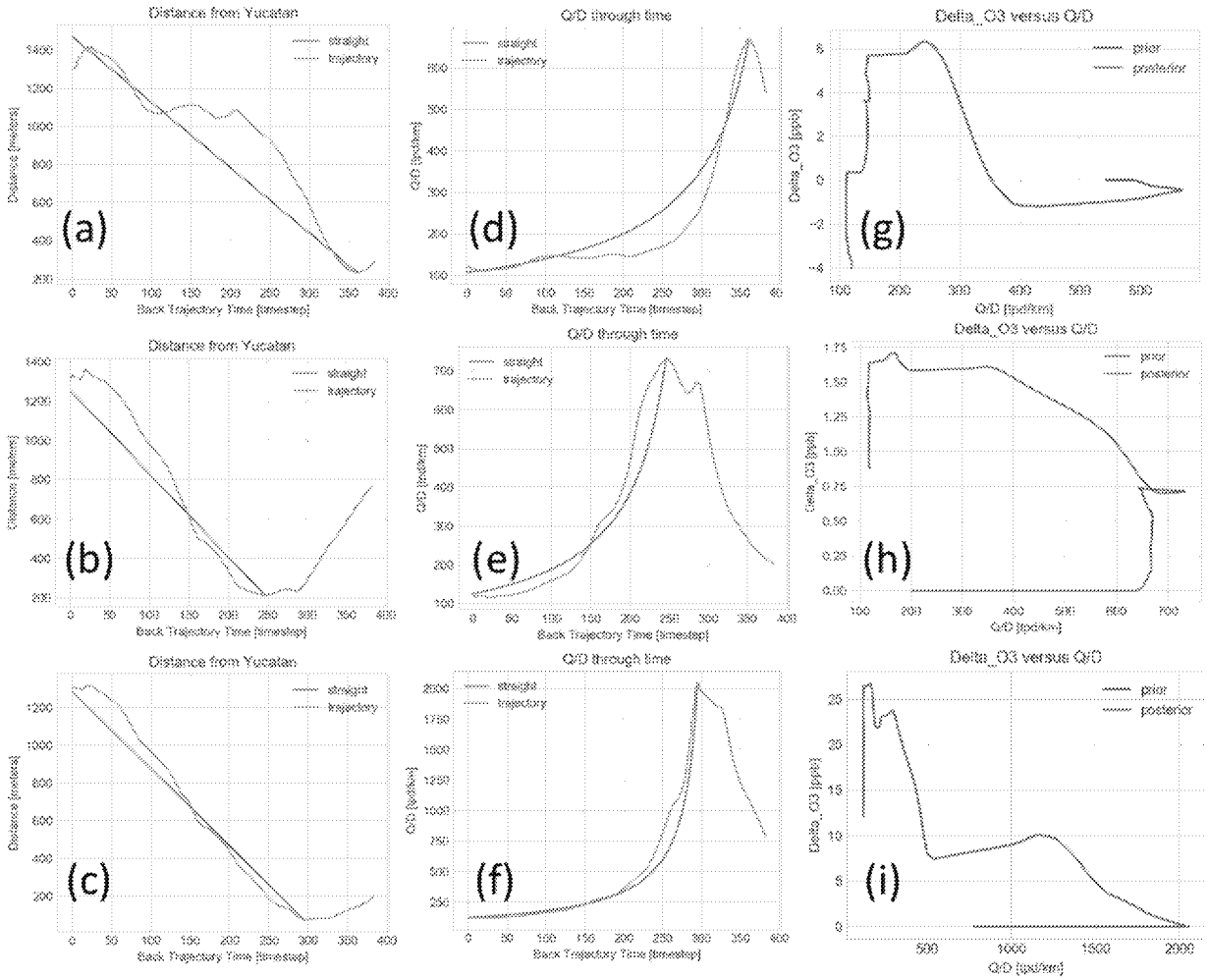

Figure 15: Distance, Q/D, and ozone enhancement for the three particles in Figure 14. The rows in this figure match the rows in Figure 14. The first column (Figure 15a, b, c) plots the distance from the Yucatan along the back-trajectory time (t=0 is the time the parcel reaches the receptor) for a straight line (blue) and along the particular trajectory (orange). The straight-line distance begins at the parcels closest approach to the Yucatan. The second column (Figure 15d, e, f) plots the Q/D metric along the back-trajectory time, and the colors are the same as those in Figures 15a, b, c. The third column plots the wildfire ozone enhancement (Delta_O3) against the Q/D metric (Figure 15g, h, i). The red lines are prior to the parcel reaching its closest approach to the Yucatan, and the green lines follow the parcel from its closest approach to the receptor.

For the first back-trajectory (Figure 14a and 15a, d, g), we can see that the parcel originated south of the Yucatan Peninsula, advected over it into the Gulf of Mexico, then passed over the East Coast of Mexico near the Mexico-US border. It then moved back over the Gulf of Mexico before moving over Texas. This meandering trajectory complicates the Q/D metric (shown by differences between the orange and blue lines in Figure 15a and 15d), which overestimates the D portion of the Q/D metric (and thus underestimates the Q/D magnitude) for much of the parcel trajectory.

Figure 15g demonstrates some of the challenges with interpreting the Q/D metric. The Q/D metric can generally be considered inversely related to time, starting during the wildfire emissions (a small D, and thus a large Q/D) and ending when the parcel reaches the receptor (a large D, and thus a small Q/D). However, as our parcel starts prior to the closest pass to the Yucatan (transition from the red line to the green line in Figure 15g), we need to consider the prior and posterior Q/D separately. After passing over the Yucatan, the parcel shows negative ozone enhancement until it reaches roughly 400 kilometers into the Gulf of Mexico (Figure 14a), where ozone enhancement up to 6 ppbv is seen (Figure 15g). During the parcel meandering over Mexico, then the Gulf of Mexico again, and then over Texas, the ozone enhancement stabilizes, drops, stabilizes, and then plummets to a negative enhancement by the time it reaches the Jones Forest monitoring station. For this case, the relevance and efficacy of using the Q/D metric to interpret ozone enhancement from wildfires is small. For parcels that follow a more straight-line trajectory between the Yucatan and Texas (see below), the Q/D metric may be more useful, although high variability is noted.

For the second back-trajectory (Figure 14b and 15b, e, h), the parcel starts out south of Cuba before passing over the tip of the Yucatan Peninsula. It then follows a relatively direct route to the Texas receptor, and the straight-ling or trajectory D and Q/D are relatively consistent (Figure 15b,e). For this parcel, little ozone enhancement is noted (< 2 ppbv), although there is some enhancement from the Yucatan wildfire emissions. As with the first parcel, ozone enhancement rises, plateaus, and then drops as the parcel travels over the Gulf of Mexico and then over land within Texas.

For the third back-trajectory (Figure 14c and 15c, f, i), the parcel originates within the Yucatan Peninsula and advects towards the Texas receptor in a largely straight line. The D and Q/D estimates are consistent between the straight-line and trajectory interpretation (Figure 15c,f). While over the Yucatan Peninsula, rapid ozone enhancement is noted (up to 10 ppbv), after which, like the other parcels, the ozone enhancement shows complicated variability: decreasing, rapidly increasing, oscillating, and then plummeting (Figure 15i).

These three example back-trajectories demonstrate that the straight-line assumption implicit in the Q/D metric does not hold for all particles (which will be further demonstrated below when all 500 back-trajectories are examined). Further, even when the back-trajectories do follow a largely straight-line route (Figure 14b,c), the impact of wildfire emissions on the ozone chemistry is highly variable. Finally, in many cases, parcels that have ozone enhancement during their back-trajectories show a rapid decrease in the ozone enhancement as the parcels reach their final receptors. Sometimes this rapid decrease results in ozone suppression rather than ozone enhancement (e.g. Figure 14a and Figure 15g).

We now turn to the three cases and interpret the 500 back-trajectory STILT-ASP simulations. We first summarize the behavior of all 500 particles, and then focus on those that passed over the Yucatan Peninsula and demonstrated significant ozone enhancement. We conclude by plotting the ozone enhancement due to wildfires (Delta_O3) against the Q/D metric for those particles and explore their ensemble and average behavior. Q, D, and Q/D estimates for these days are in Table 3 – note that these cases would qualify for the Tier 2 level of demonstration under the current Q/D approach.

Table 3: Q, D, and Q/D estimates for the Yucatan Peninsula for the cases examined here.

	Q [tpd]	D [km]	Q/D [tpd/km]
26-Apr-11	158,800	1,000	159
27-Apr-11	265,000	1,000	265
30-Apr-13	140,000	1,000	140
1-May-13	157,000	1,000	157
2-May-13	244,000	1,000	244

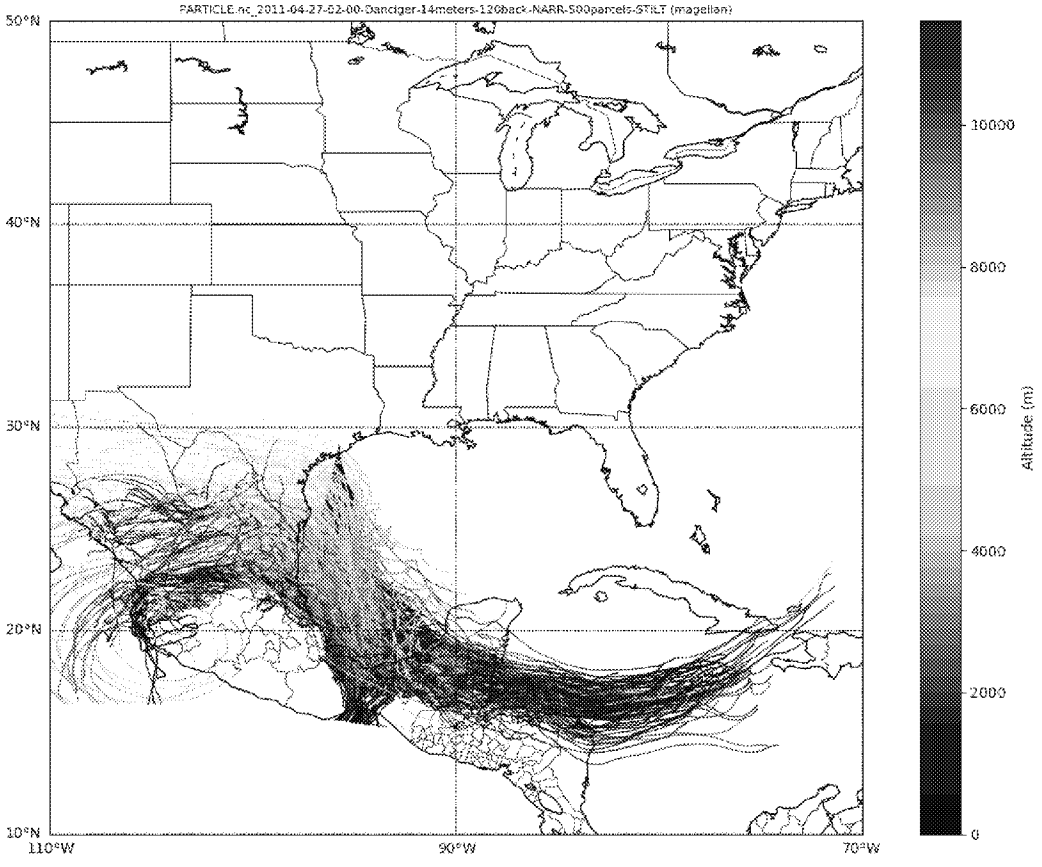

Figure 16: Five-day back trajectories for 500 parcels from the Danciger monitoring site in HGB on April 27, 2011 at 02:00 UTC (21:00 CST on April 26, 2011) demonstrating influence of Yucatan fires on this date.

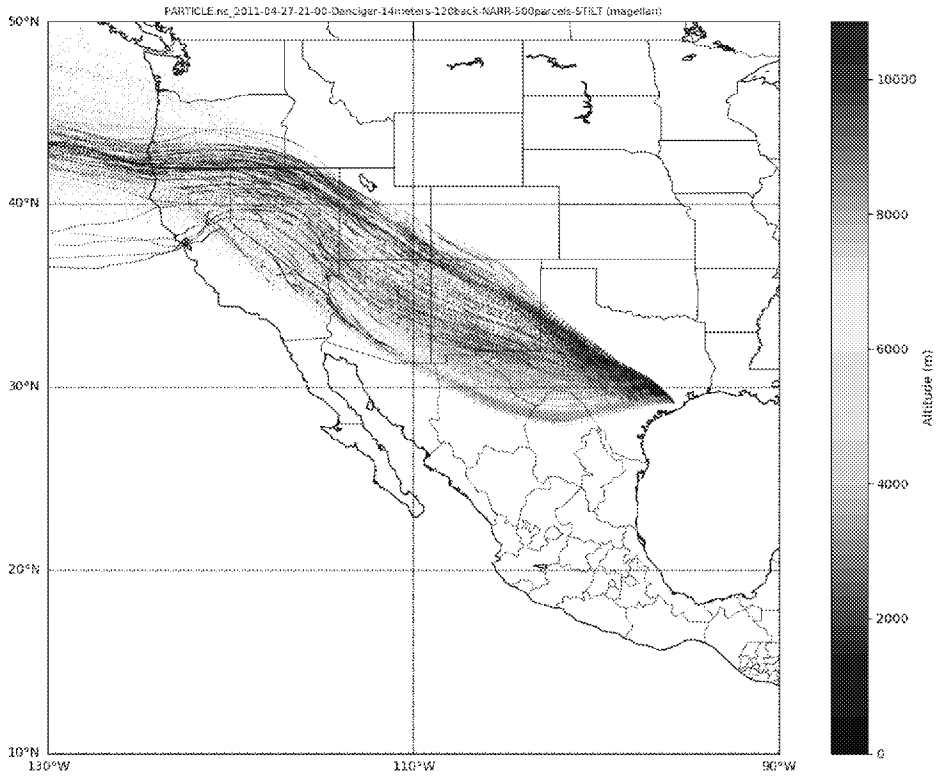

Figure 17. Five-day back trajectories from the Danciger monitoring site in HGB on April 27, 2011 at 21:00 UTC, showing that the site was unaffected by Yucatan fires on this date.

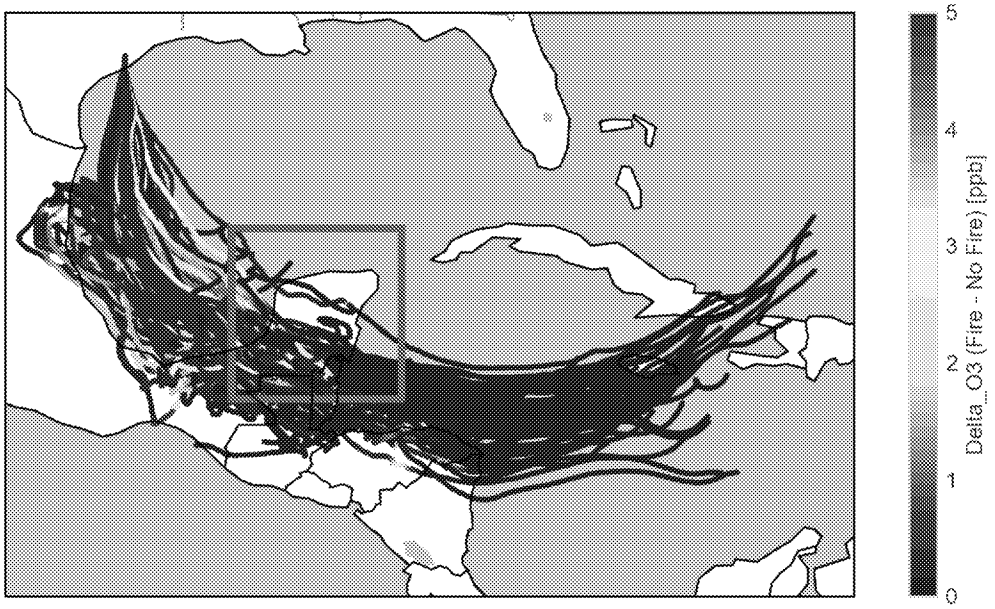

Figure 18: Five-day back trajectories for parcels from the Danciger monitoring site on April 26, 2011 that pass through the Yucatan region (red box) and have a fire-influenced ozone value (Delta_O3, color bar) of at least 1 ppbv during some part of the back trajectory. Of the 500 back-trajectories, 181 pass over the Yucatan and 139 of those exceed 1 ppbv.

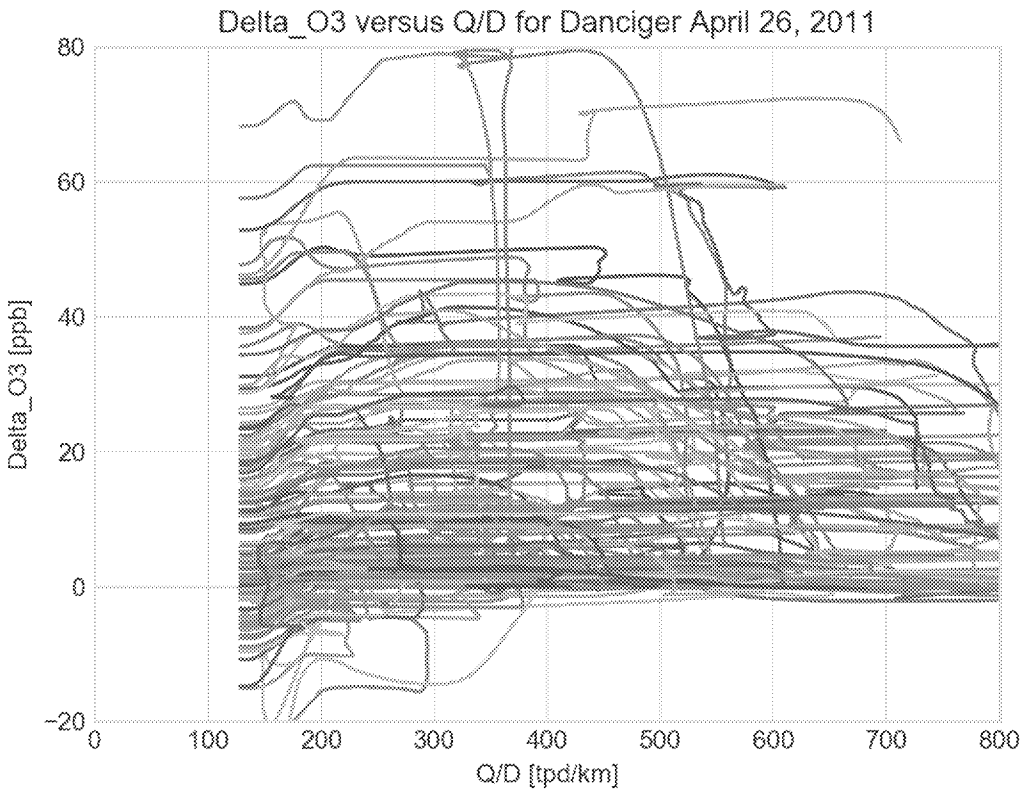

Figure 19: Plot for the Danciger site on April 26, 2011 of the fire-influenced ozone enhancement (Delta_O3, y-axis) versus the Q/D metric for the parcels that pass through the Yucatan region (red box) and have a fire-influenced ozone value (Delta_O3) of at least 1 ppbv during some part of the back trajectory. Of the 500 back-trajectories, 181 pass over the Yucatan and 139 of those exceed 1 ppbv. The distances used to calculate the D in the Q/D metric follow the parcel trajectories from the closest pass to the center of the Yucatan peninsula to the Danciger site. The colors of each back-trajectory are arbitrary.

On April 26, 2011, roughly a third of the back-trajectories originating in from the Danciger (C618) monitoring station passed over the Yucatan Peninsula reached the Texas coast and passed over the Houston-Galveston-Brazoria (HGB) region (Figure 16). Some of the other monitoring stations in the HGB region measured hourly ozone mixing ratios exceeding 45 ppbv, although generally ozone values remained low (< 40 ppbv). The ozone within parcels that passed over the Yucatan Peninsula were moderately enhanced by wildfire emissions (Figure 18), although a look at the ozone enhancement relative to the Q/D metric (Figure 19) shows that only a small number of particles maintained high ozone enhancement by the time they reached the Danciger monitoring station. Many parcels showed little-to-no (< 5 ppbv) ozone enhancement and roughly 20 – 25 of the parcels show negative ozone enhancement by the time they reached the Danciger monitoring station. On average, wildfire ozone enhancement at the Danciger monitoring station was small. The difference between a STILT-ASP run with wildfire emissions and without fire emissions averaged over all 500 particles is 1.8 ppbv ozone. At the receptor, the average of the parcels that passed over the Yucatan Peninsula and demonstrate positive ozone enhancement during some point of their trajectory (see Figure 18 and Figure 19) is 11.4 ppbv.

The following day, April 27, 2011, many monitoring stations within the HGB region measured high hourly ozone mixing ratios (< 70 ppbv), largely in the afternoon (13:00 – 1600 CST). However, unlike the previous day, back trajectories of all 500 particles approach the Danciger monitoring station from the west (Figure 17). Many of the parcels passed through low-altitude (< 2,000 meter) portions of Oregon, California, Nevada, Utah, Arizona, and New Mexico, with other particles originating in the free troposphere (2,000 – 10,000 meters) over the Pacific Ocean (Figure 17).

On the afternoon of May 1, 2013, high ozone mixing ratios (> 80 ppbv) were measured within the HGB region, with a maximum value of 88 ppbv measured at the Jones Forest (C698) monitoring station at 16:00 CST. Back trajectories (Figure 20) show most of the air parcels reaching the Jones Forest monitoring station originated within the Gulf of Mexico, with some originating eastward of Cuba. As shown in Figure 22, only a small number of these parcels passed over the Yucatan region (178 of 500 parcels), and of these, only a small number showed any ozone enhancement in excess of 1 ppbv (38 of 500 particles). Figure 24 plots the ozone enhancement for these 38 particles as a function of the Q/D metric, and while some parcels show significant ozone enhancement (up to 30 ppbv ozone), many parcels show little-to-no ozone enhancement (< 5 ppbv), while a few show negative ozone enhancement by the time the parcels reach the Jones Forest monitoring station. On average, ozone enhancement due to wildfires from all 500 particles is negligible. At the receptor, the average of the parcels that passed over the Yucatan Peninsula and demonstrate positive ozone enhancement during some point of their trajectory (see Figure 22 and Figure 24) is 3.9 ppbv.

The following day, May 2, 2013, the HGB region had low background levels of ozone (< 30 ppbv), although some hours in the early afternoon exceeded 40 ppbv hourly ozone. Back trajectories (Figure 21) show that most of the air that reached the Jones Forest monitoring station originated within the Gulf of Mexico and the Atlantic Ocean. Half of the 500 back trajectory parcels passed near or over the Yucatan Peninsula (Figure 23), and 59 of these showed ozone enhancements in excess of 1 ppbv. Figure 25 again plots the ozone enhancement due to wildfires versus the Q/D metric, and as in the previous cases, we see that most of the parcels show little-to-no ozone enhancement (< 10 ppbv), although some due show significant ozone enhancement (up to 40 ppbv) due to the Yucatan region wildfires. On average, the wildfire influence on ozone enhancement within Jones Forest on May 2, 2013 was around 10 ppbv, which, due to the low background levels of ozone did not exceed the regulatory standards for ozone on that day. At the receptor, the average of the parcels that passed over the Yucatan Peninsula and demonstrate positive ozone enhancement during some point of their trajectory (see Figure 23 and Figure 25) is 1.3 ppbv.

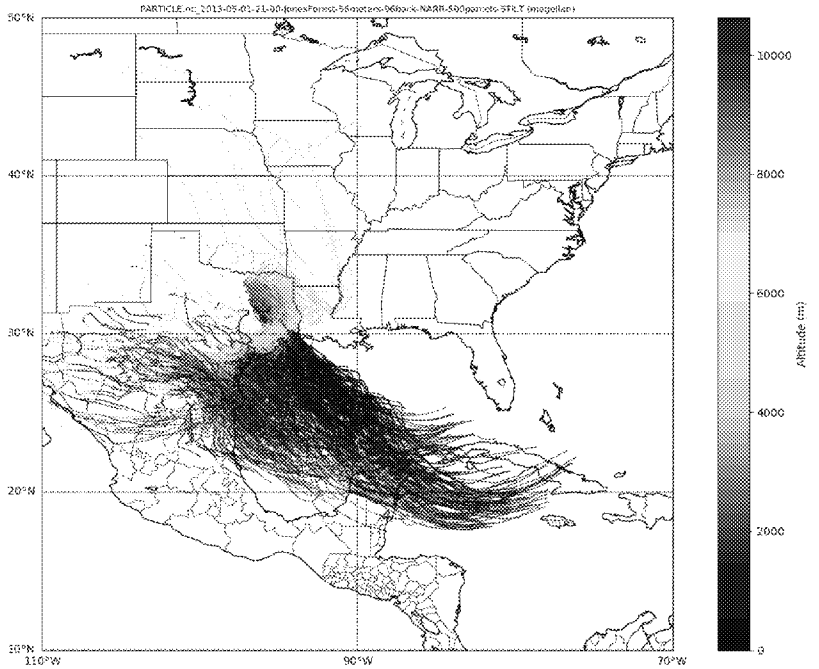

Figure 20: Four-day back trajectories for 500 parcels from the Jones Forest monitoring site in HGB on May 1, 2013 at 21:00 UTC demonstrating influence of Yucatan fires on this date.

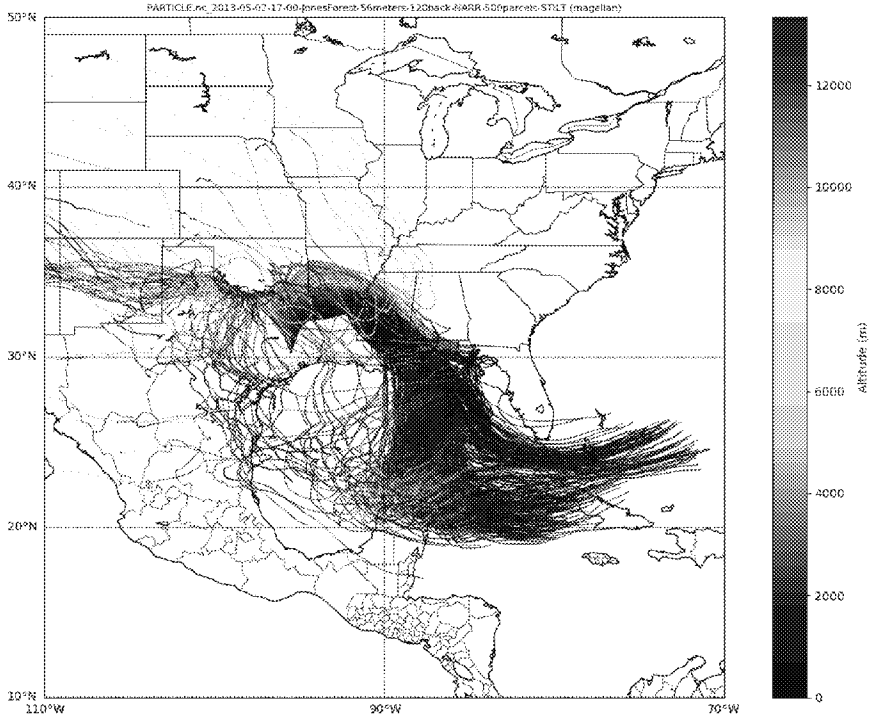

Figure 21: Five-day back trajectories for 500 parcels from the Jones Forest monitoring site in HGB on May 2, 2013 at 17:00 UTC demonstrating influence of Yucatan fires on this date.

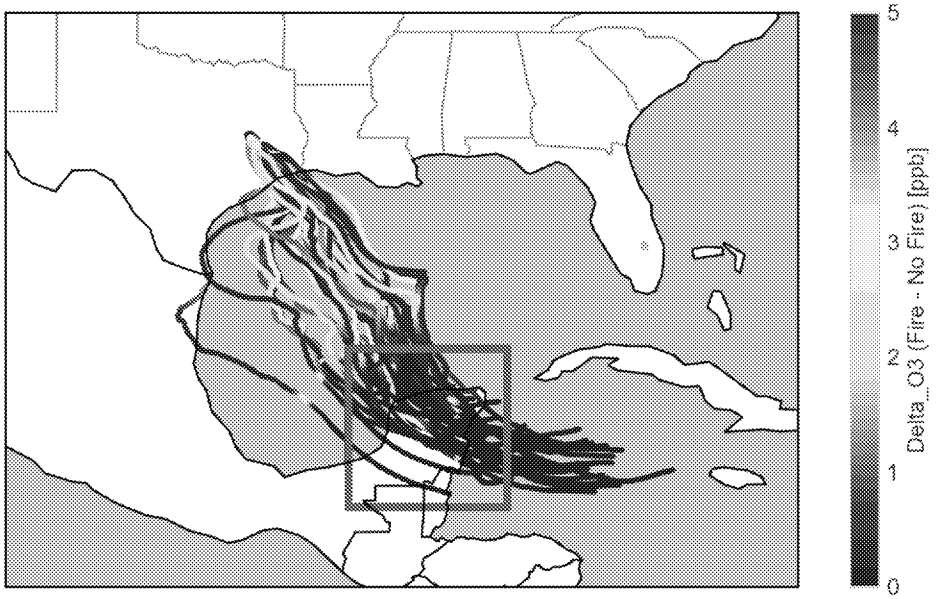

Figure 22: Four-day back trajectories for parcels from the Jones Forest monitoring site on May 1, 2013 that pass through the Yucatan region (red box) and have a fire-influenced ozone value (Delta_O3, color bar) of at least 1 ppbv during some part of the back trajectory. Of the 500 back-trajectories, 178 pass over the Yucatan and 38 of those exceed 1 ppbv.

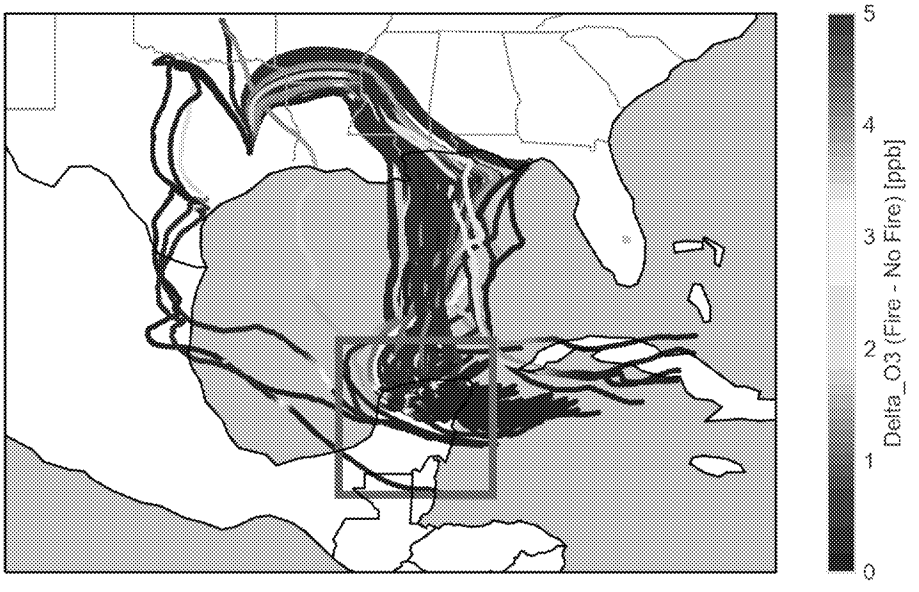

Figure 23: Five-day back trajectories for parcels from the Jones Forest monitoring site on May 2, 2013 that pass through the Yucatan region (red box) and have a fire-influenced ozone value (Delta_O3, color bar) of at least 1 ppbv during some part of the back trajectory. Of the 500 back-trajectories, 250 pass over the Yucatan and 59 of those exceed 1 ppbv.

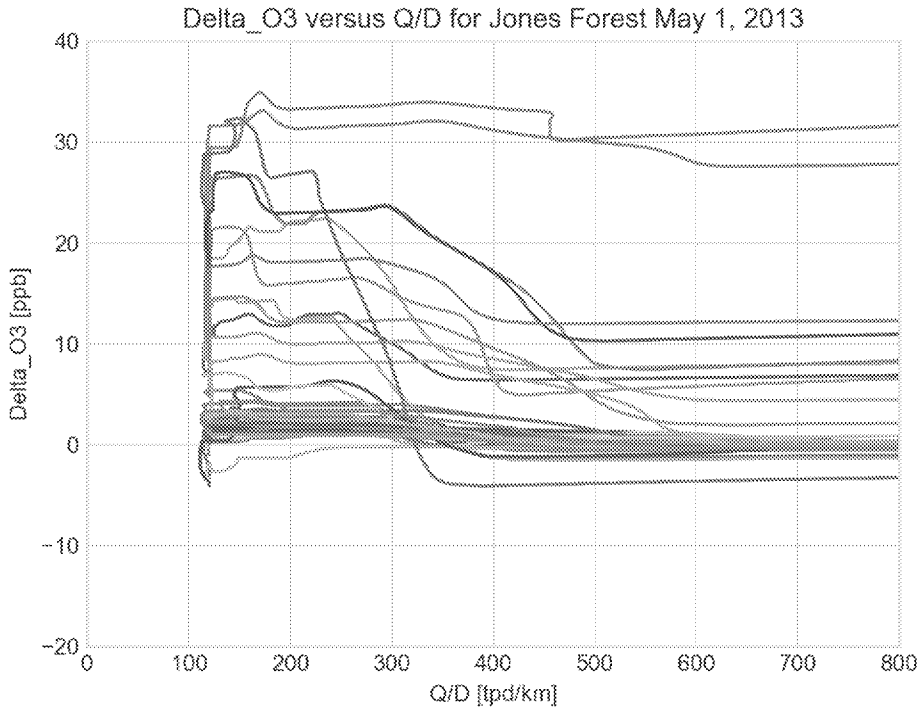

Figure 24: Plot for the Jones Forest site on May 1, 2013 of the fire-influenced ozone enhancement (Delta_O3, y-axis) versus the Q/D metric for the parcels that pass through the Yucatan region (red box) and have a fire-influenced ozone value (Delta_O3) of at least 1 ppbv during some part of the back trajectory. Of the 500 back-trajectories, 250 pass over the Yucatan and 59 of those exceed 1 ppbv. The distances used to calculate the D in the Q/D metric follow the parcel trajectories from the closest pass to the center of the Yucatan peninsula to the Jones Forest site. The colors of each back-trajectory are arbitrary.

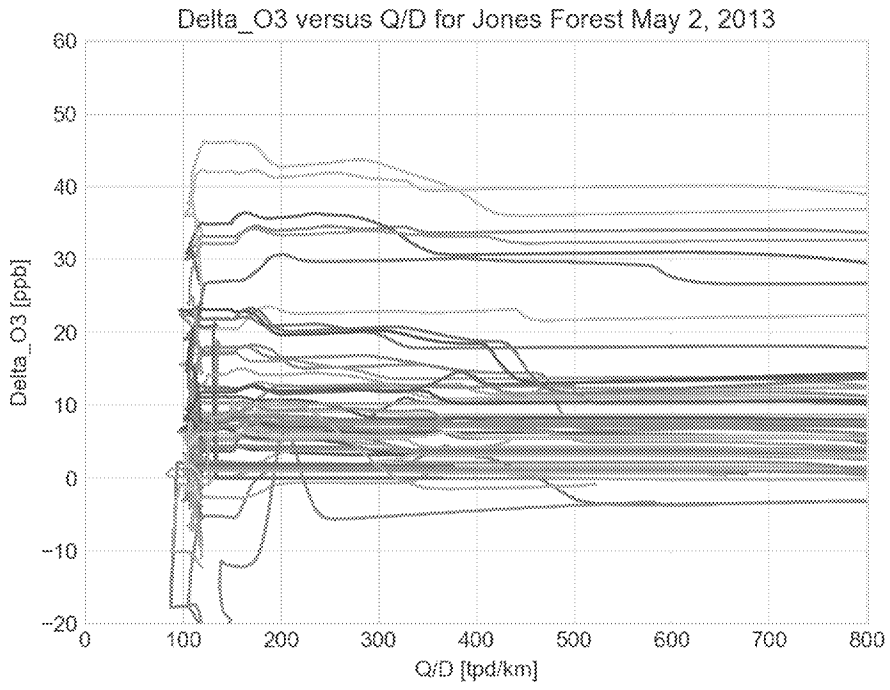

Figure 25: Plot for the Jones Forest site on May 2, 2013 of the fire-influenced ozone enhancement (Delta_O3, y-axis) versus the Q/D metric for the parcels that pass through the Yucatan region (red box) and have a fire-influenced ozone value (Delta_O3) of at least 1 ppbv during some part of the back trajectory. Of the 500 back-trajectories, 178 pass over the Yucatan and 38 of those exceed 1 ppbv. The distances used to calculate the D in the Q/D metric follow the parcel trajectories from the closest pass to the center of the Yucatan peninsula to the Jones Forest site. The colors of each back-trajectory are arbitrary.

3.3 GAM Residual Analysis

Recent work by Gong et al. (2017) has suggested that statistical models that relate MDA8 O_3 concentrations to meteorological variables can be used to estimate the impact of fires on O_3 in urban areas. The idea is that a generalized additive model (GAM; Wood, 2006) can be developed to predict the MDA8 O_3 concentration in an urban area using historical data. The impact of fires on the MDA8 O_3 during fire events (established with back trajectories) can then be estimated from the difference between the observed MDA8 O_3 and the GAM-predicted value (i.e., the model residual). However, as the GAMs are inherently statistical, some error in the model predictions is expected even on days with no fire influence, and thus it is difficult to separate the impacts of statistical noise from rare events such as biomass burning impacts.

We evaluated this GAM technique for the May 1-2, 2013 event in HGB using our previously developed GAM models for HGB (Pernak et al., 2017). The April 26-27, 2011 event was not analyzed as our GAMs for HGB only cover the May to October "ozone season."

On May 1, 2013, the GAM residual was 2.8 ppbv. This would imply a fire impact of 2.8 ppbv if the error was all due to the Yucatan fire impact on O_3. However, the standard deviation for the GAM predictions is around 10 ppbv, and thus a difference of 2.8 ppbv is well within the expected statistical noise for the technique. Similarly, the fire impact estimated via the GAM for

May 2, 2013 (4.0 ppbv) is well within the expected statistical noise for the GAM models. Therefore the GAMs provide weak evidence for a fire impact of about 3-4 ppbv during this event.

4 Assessing Q/D During Biomass Burning Events Impacting El Paso

On June 21, 2015, the El Paso University of Texas at El Paso (UTEP) (CAMS 12) monitoring site measured a maximum daily eight-hour ozone average of 77 parts per billion (ppbv). These measurements were elevated by emissions from the Hog fire in southeastern Arizona, which were transported approximately 155 miles across the deserts of New Mexico and Mexico before entering the El Paso area from south (TCEQ, 2016). Additional fires in eastern Arizona also contributed emissions (Table 4). The VOC and NOx emissions from these fires are summarized in Table 5, showing that the Q/D values for these fires were low (< 1 tpd/km) and so would not have qualified for a Tier 2 level of demonstration. Our analysis focuses on the Hog fire and the largest of the secondary fires, the Whitetail Complex fire.

Using CAMx inputs and outputs provided by TCEQ, we used the CAMx model to analyze this potential exceptional event in El Paso, Texas and analyze the consistency between the CAMx modeling results and the Q/D metric (Section 4.1). We also analyzed this event using the ASP (Section 4.2) and STILT-ASP (Section 4.3) models, similar to the analysis done for the HGB fire events in Section 3.

Table 4. Fires Contributing to El Paso Exceptional Event. Reproduced from TCEQ (2016).

Fire Name	Location (Lat/Lon)	Size (acres)	Cause	Start Date	End Date
Hog Fire	31.503 °N 109.089 °W	8,000	Lightning	6/17/2015	6/25/2015
Whitetail Complex	33.574 °N 110.246 °W	33,633	Lightning	6/16/2015	6/29/2015
Sawmill	33.507 °N 109.932 °W	5,667	Lightning	6/17/2015	6/29/2015
Kearney River	33.050 °N 110.917 °W	1,428	Human	6/17/2015	6/27/2015
Saguaro	32.340 °N 109.784 °W	119	Human	6/18/2015	6/20/2015

4.1 CAMx Simulations

We analyzed the 4-km resolution CAMx output for June 2015 provided by the TCEQ to see if the modeled impact of the fires in Table 4 on El Paso during the June 21, 2015, Exceptional Event is consistent with the Q/D metric. This output included simulations with and without fire emissions and included an 8-hour running average for O_3.

We focused our analysis on the time period of the maximum MDA8 O_3 detected in El Paso on June 21, 2015. The impact of fires on O_3 in this period is shown in Figure 26. The largest impact of fires on O_3 at the north of the 4-km domain is from a fire that did not impact El Paso, and so we filtered out these impacts in our analysis below by excluding all results north of 35 °N. The fires in southern Arizona in Table 4 resulted in impacts of 9-15 ppbv in the El Paso area.

Table 5. FINN emissions of VOC and NO_x from the El Paso fires, as well as Q-values (Q = VOC + NO_x), an estimate of D, and Q/D values. We include estimates of Q and Q/D for both a single day and a 2-day cumulative estimate to demonstrate the sensitivity of the Q/D metric to how one estimates the Q-values.

	VOC [tpd]	NOx [tpd]	Q [tpd]	2-day Q [tpd]	D [km]	Q/D, 1-day [tpd/km]	Q/D, 2-day [tpd/km]
21-Jun	89	7	96	188	250	0.384	0.752
20-Jun	85	7	92	176	250	0.368	0.704
19-Jun	78	6	84	195	250	0.336	0.78
18-Jun	103	8	111	173	250	0.444	0.692
17-Jun	57	5	62	94	250	0.248	0.376
16-Jun	30	2	32		250	0.128	

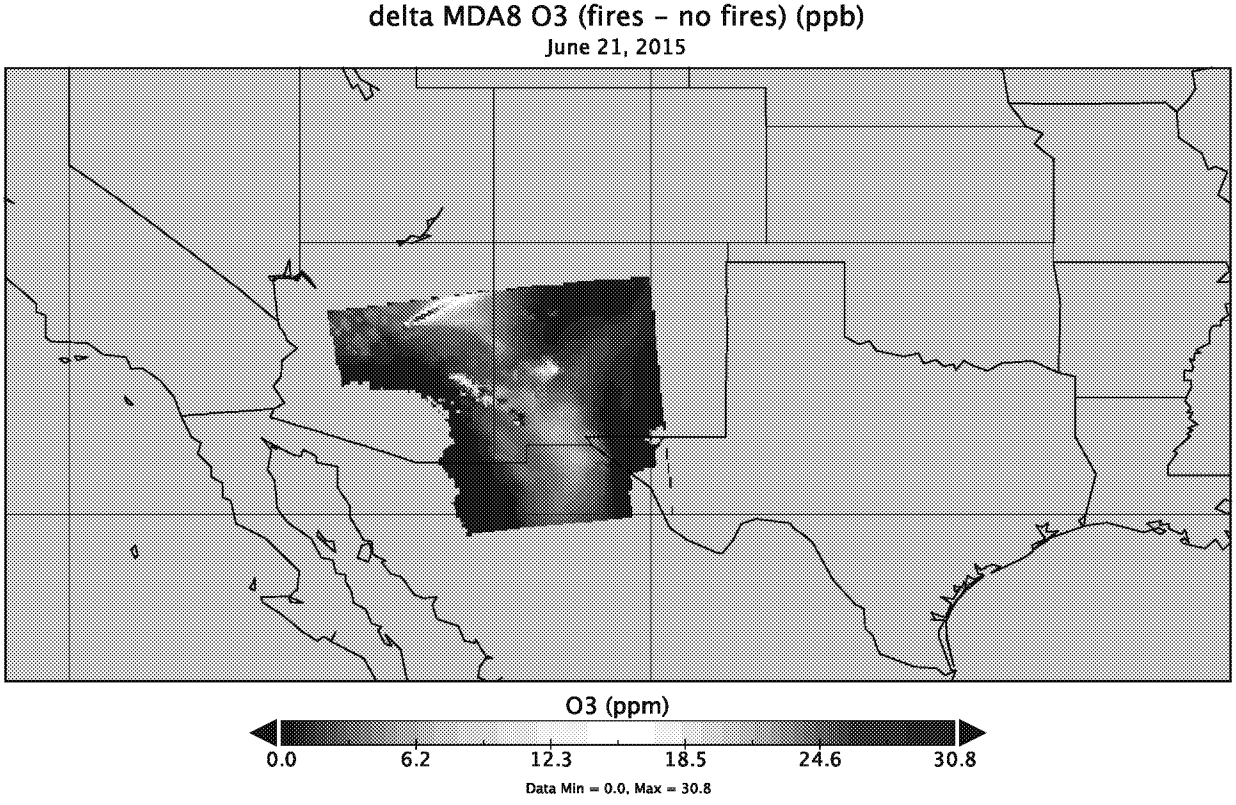

Figure 26. CAMx simulation of the impact of fires on maximum 8-hour average O_3 on June 21, 2015. Gray areas are areas where there was no data or no difference between the "with fire" and "without fire" simulations.

In order to assess if the impacts estimated by CAMx are consistent with the Q/D metric, we averaged the ozone impact results in Figure 26 in terms of the distance from the Hog Fire and the Whitetail Complex fire. We binned the results for every 4 km of distance from the fires and calculated the average fire O_3 impact for each bin. We then analyzed these average results in terms of distance and the reciprocal of distance.

Figure 27 shows the average fire O_3 impact on MDA8 O_3 versus distance from the Hog fire. Rather than steadily decreasing with distance as expected from the Q/D metric, we can see that the O_3 impact of fires increases with distance from the Hog Fire, with the impact peaking at the distance of El Paso (~175 km) and further downwind. This peak could be due to either O_3 production in the Hog fire plume itself, or the additional impact of the plume from the Whitetail complex fire, or could represent an increase in O_3 formation as the new NO_x emissions from the El Paso-Ciudad Juárez area mixes with the VOC-rich fire emissions, which would explain why the maximum impacts are slightly downwind of El Paso.

Figure 28 shows the same results plotted in terms of the reciprocal of distance from the Hg fire. In this framework, the impacts on O_3 are relatively constant at 1.5 ppbv with inverse distance from the fire except for the peak near the 175-225 km distance downwind. This suggests that there is both an initial burst of O_3 production that is consistent with the Q/D metric, but there is a secondary production process further downwind that leads to additional O_3 production, and thus the overall impacts are not consistent with the Q/D metric.

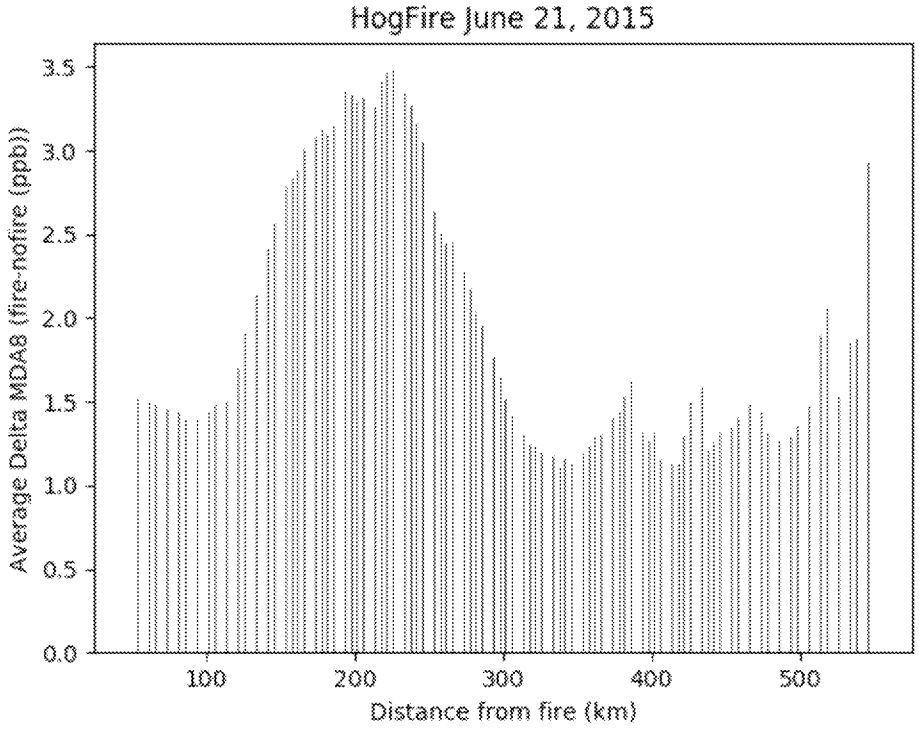

Figure 27. CAMx calculated fire impacts on MDA8 O_3 versus distance from the Hog Fire on June 21, 2015. Results were binned every 4 km and the average value for each bin is plotted.

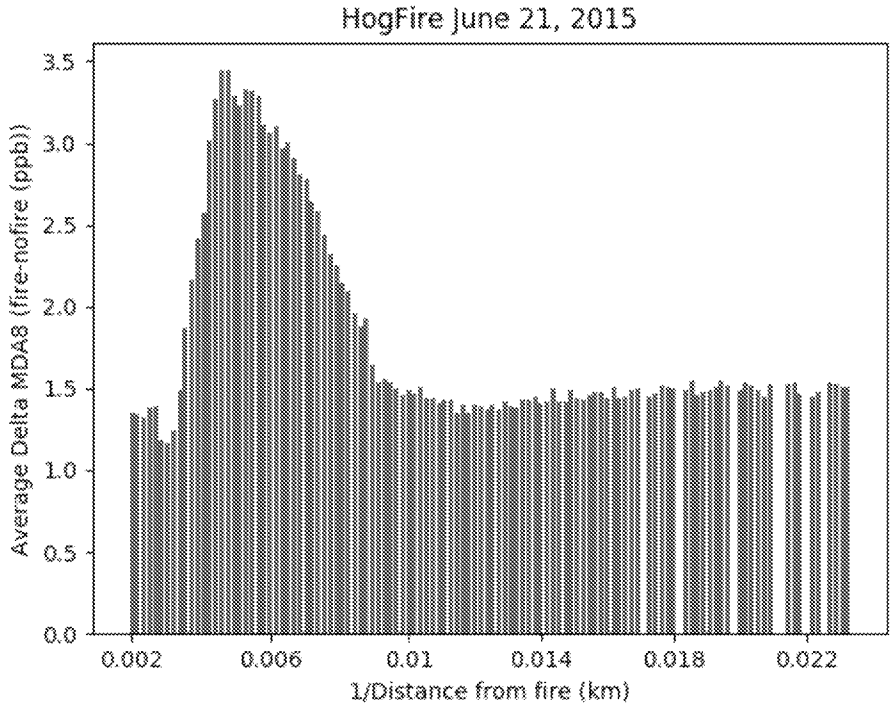

Figure 28. As in Figure 27, but plotted versus the reciprocal of distance.

Figure 29 shows the average fire O_3 impact on MDA8 O_3 versus distance from the Whitetail Complex fire. There is a steady increase out to about 325 km, with a secondary peak at about 150 km – the secondary peak could be due to interactions with the Hog Fire plume. After 325 km, the O_3 impact decreases with distance suggesting that this is due to dispersion of the O_3 formed upwind. This suggests that the Q/D metric would work for this fire at distances greater than 325 km, but the dependence within 325 km of the fire is the opposite of that implied by the Q/D metric.

Figure 30 shows the same results plotted in terms of the reciprocal of distance from the Whitetail Complex fire. It is clear that the impacts on O_3 are not constant with inverse distance from the fire, but are much more consistent with steady O_3 production in the plume followed by dilution at large distances

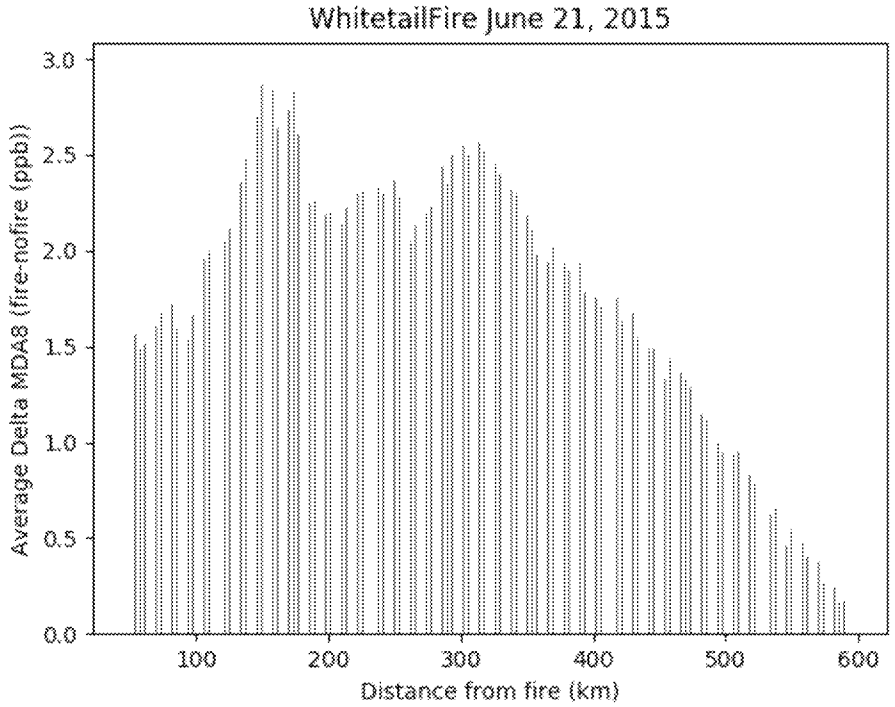

Figure 29. CAMx calculated fire impacts on MDA8 O_3 versus distance from the Whitetail Complex Fire on June 21, 2015. Results were binned every 4 km and the average value for each bin is plotted.

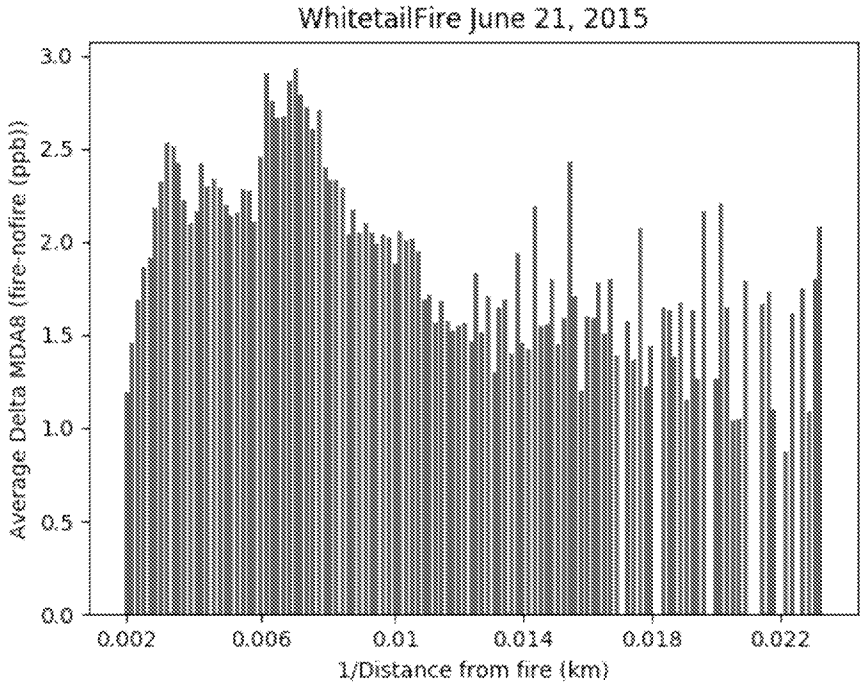

Figure 30. As in Figure 29, but plotted versus the reciprocal of distance.

4.2 ASP Simulations

We used the ASP model to investigate the dependence of the O_3 formation in the Hog Fire and Whitetail Complex fire plumes with time after emission from the fire as a proxy for the dependence on distance from the fire. As in Section 3.1, our goal here is not to accurately estimate the fire impacts on O_3 in El Paso, but rather to see if the modeled formation of O_3 downwind of the fire is consistent with the Q/D metric.

ASP v2.1.1 was set up in a similar fashion as discussed in Section 3.1. The major difference for these fires is that their small size relative to the combined Yucatan fire plume means that dilution of the plume will be an important factor in its evolution. We assume initial plume widths of 2 km with horizontal eddy diffusivities of 10^4 m^2/s, consistent with values previously derived for the similarly sized Timbavati fire in Alvarado et al. (2009). This gives an initial mixing timescale of 100 s, so there will be a rapid initial dilution of the plume that decrease as the plume grows.

Based on El Paso observation on June 21, 2015, we assumed an average temperature of 305 K and relative humidity of 10%. Pressure was held constant at 950 hPa. Cloud-free photolysis rates were calculated with TUV v5.0 for June 21, 2015 at approximately the latitude of El Paso (31.75 ^oN) without accounting for any impact of the aerosols on the photolysis rates.

The FINN inventory gives the area of the Hog Fire as 0.69 km^2, with a CO emission rate of $1.12x10^6$ mol CO/day. Assuming a vertical mixing height of 2 km and that the parcel picks up 8% of the total emissions before transporting downwind gives a value of ΔCO_{init} of ~2000 ppbv, but to account for uncertainties in this value we simulated 1000 ppbv and 4000 ppbv as well. The

Whitetail complex fire has a very similar ΔCO_{init} value of 1800 ppbv (calculated with the FINN area of 0.78 km^2 and the CO emission rate of $1.41x10^6$ mol CO/day), and so one ASP simulation can be representative of both fires. Both fires are identified as "Woody Savannah/Shrublands" by FINN, and so we use the emission factors for grasslands/savannahs from Akagi et al. (2011).

4.2.1 Sensitivity to Emissions and PBL Heights

Figure 31 shows the enhancement of CO and O_3 in the ASP-simulated Hog fire plume for the three different values of ΔCO_{init} tested. In this baseline simulation, all plumes were initially emitted at local noon. We can see that the con centration of O_3 rapidly increases in the first six hours after emission as chemical production of O_3 is greater than the reduction due to plume dilution. However, after six hours dilution is greater than the nighttime O_3 production and the O_3 enhancement in the plume decreases, except for a small increase around noon on the second day. Thus while the O_3 enhancement does decrease with distance after the first six hours in this case, the behavior during the rapid increase is not consistent with the Q/D metric. However, the O_3 enhancement is roughly proportional to the value of ΔCO_{init}, suggesting that the O_3 production is proportional to the fire emissions if other parameters (fire area and mixing height) are held constant.

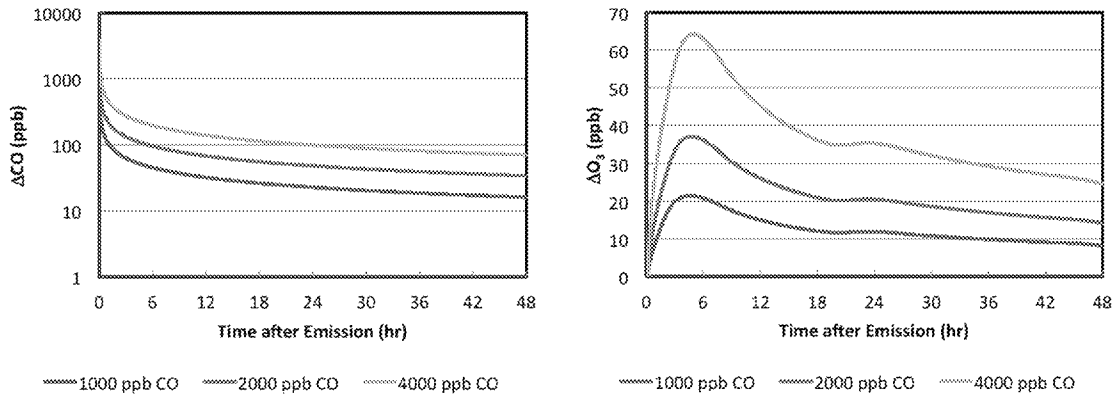

Figure 31. Modeled fire enhancement of CO (left) and O_3 (right) versus time after emission for the Hog fire simulation with different values of ΔCO_{init}.

One potential alternate screening metric would be to use literature values of the enhancement of O_3 in biomass burning plumes relative to the enhancement in CO ($\Delta O_3/\Delta CO$), and then multiply this value by model predictions of the transport of fire CO. This would be simpler than a Tier 3 demonstration in that it would not require photochemical modeling, but would be more consistent with the literature (e.g., Jaffe and Wigder, 2013). Figure 32 shows the ASP simulation results from Figure 31 plotted in terms of $\Delta O_3/\Delta CO$ versus time. This suggests that this approach would also have trouble representing the initial rapid production of O_3 in the plumes, but that it would be a reasonable screening approach further downwind where this value settles into a relatively constant value, but still has some dependence on the value of ΔCO_{init}..

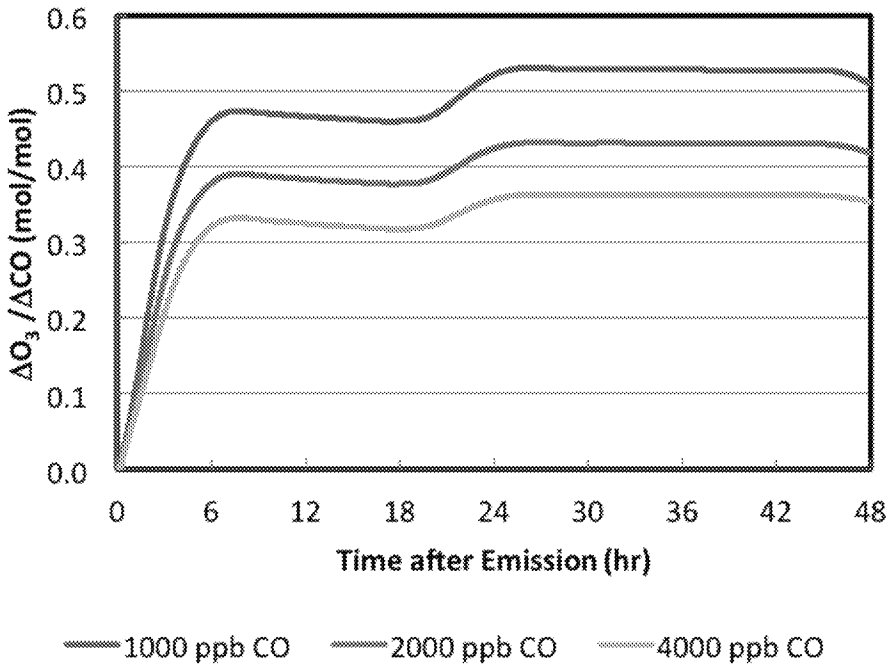

Figure 32. Ratio of O_3 enhancement to CO enhancement in the Hog Fire plume as a function of time after emission for different values of ΔCO_{init}.

4.2.2 Sensitivity to Emission Time of Day

Figure 33 shows how the fire O_3 enhancement versus time changes with different initial emission times. As expected, the initial values of the enhancement are negative, as the NO emitted from the fires titrates the background O_3. For plumes emitted at night, this negative enhancement persists for several hours before rapid O_3 production takes place after sunrise. Interestingly, while this can affect the peak O_3 enhancement, after 24 hours all of the plumes have settled into similar O_3 enhancements.

At an average wind speed of 7 miles per hour, El Paso would be about 16 hours downwind of the Hog fire. Given the peak O_3 values at the CAMS 12 site occurred at 13:00 LST, that would suggest that the plume was emitted at around 21:00 LST, corresponding to the purple curve in Figure 33. At 16 hours downwind, the purple curve implies an O_3 enhancement of 20 ppbv, higher than the CAMx prediction of ~12 ppbv in Section 4.1 but within a similar range given the uncertainties in the model inputs. The higher ASP value may be due to uncertainties in our estimates of ΔCO_{init} and the initial size and mixing timescale of the plume, which in past ASP studies were constrained by observations of the rate of decay of CO (e.g., Alvarado et al., 2015). In addition, our simulations here do not include the rapid loss of NO_x to organic nitrates due to S/IVOC chemistry in the first 5 hours notes by Alvarado et al. (2015), as we have found that our implementation of this chemistry causes too much NO_x, and thus O_3, loss further downwind (Lonsdale et al., 2017). However, as our goal here is to examine how the predicted O_3 enhancement varies with Q and D, not to predict the exact value for this event, we did not tune our simulation inputs to better match the CAMx predictions or the El Paso observations.

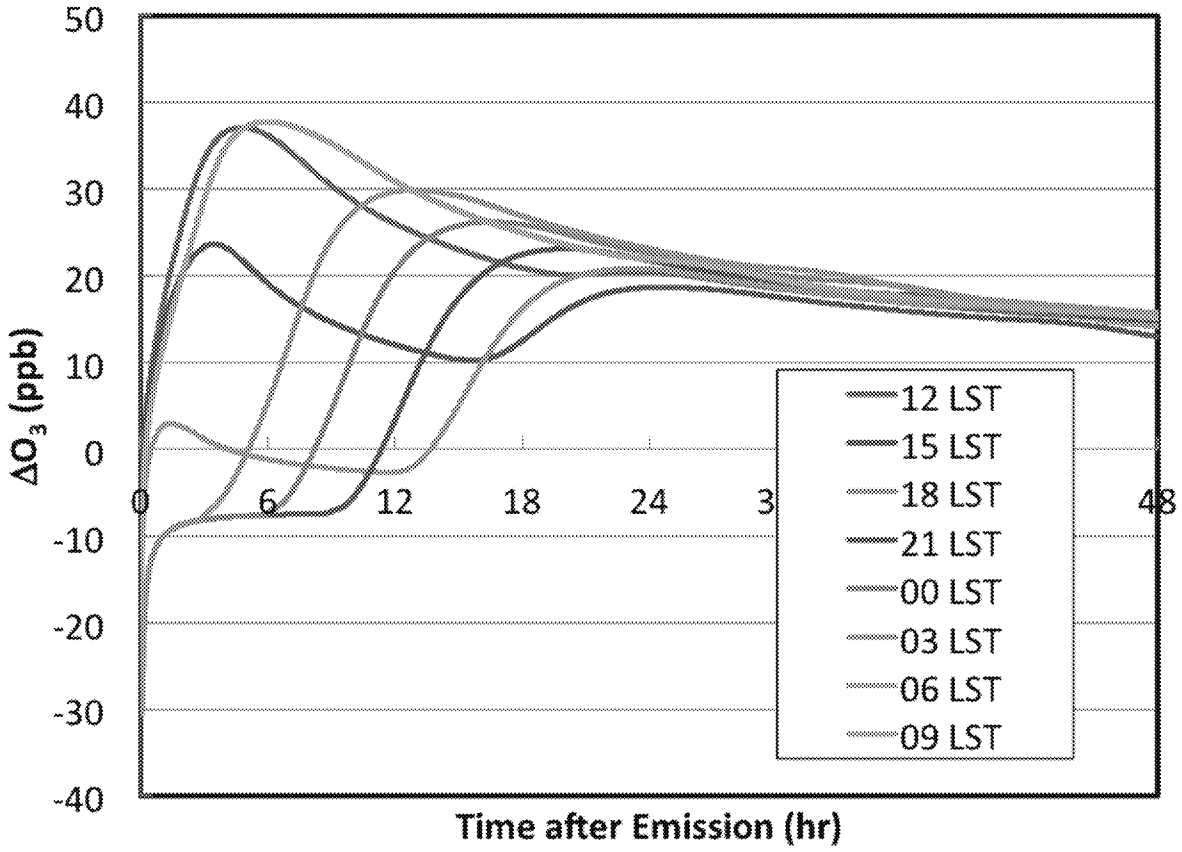

Figure 33. Fire enhancement of O_3 versus time after emission for different initial emission times for the Hog Fire. All simulations have ΔCO_{init} = 2000 ppbv as in the baseline simulation.

4.3 STILT-ASP Simulations

On June 21, 2015, hourly ozone values in the El Paso-Juárez region exceeded 75 ppbv at three sites, reaching a maximum of 97 ppbv at the El Paso UTEP (CAMS12) monitoring site at 12:000 CST. Back trajectories (Figure 34) show that air parcels reaching the El Paso UTEP monitoring site originated throughout the Southwestern United States and Northwestern Mexico, as well as out over the Pacific Ocean. As with the Yucatan Peninsula cases above, we defined a wildfire region and isolated the parcels that passed over that region and that exceeded 1 ppbv ozone enhancement due to the wildfire influence. Of the 500 back-trajectory particles, nearly all (484 of 500) pass over the fire region, but only 20 of them exceed 1 ppbv ozone enhancement from the fires (Figure 35). The overall impact of fires, determined by comparing a STILT-ASP run with fire emissions and a run without fire emissions, is negligible. At the receptor, the average of the parcels that passed over the Arizona fire region and demonstrate positive ozone enhancement during some point of their trajectory (see Figure 35 and Figure 36) is 1.94 ppbv.

Comparing the ozone enhancement and the Q/D metric (Figure 36) does not show much ozone enhancement for this period. In addition, several of the parcels appear to follow the Q/D metric, but there are still a few that show enhanced O_3 downwind, inconsistent with the Q/D metric. This low value for ozone enhancement relative to the CAMx (Section 4.1) and ASP (Section 4.2)

runs may be due to issues with the S/IVOC chemistry in STILT-ASP leading to too rapid NO_x loss (Lonsdale et al., 2017).

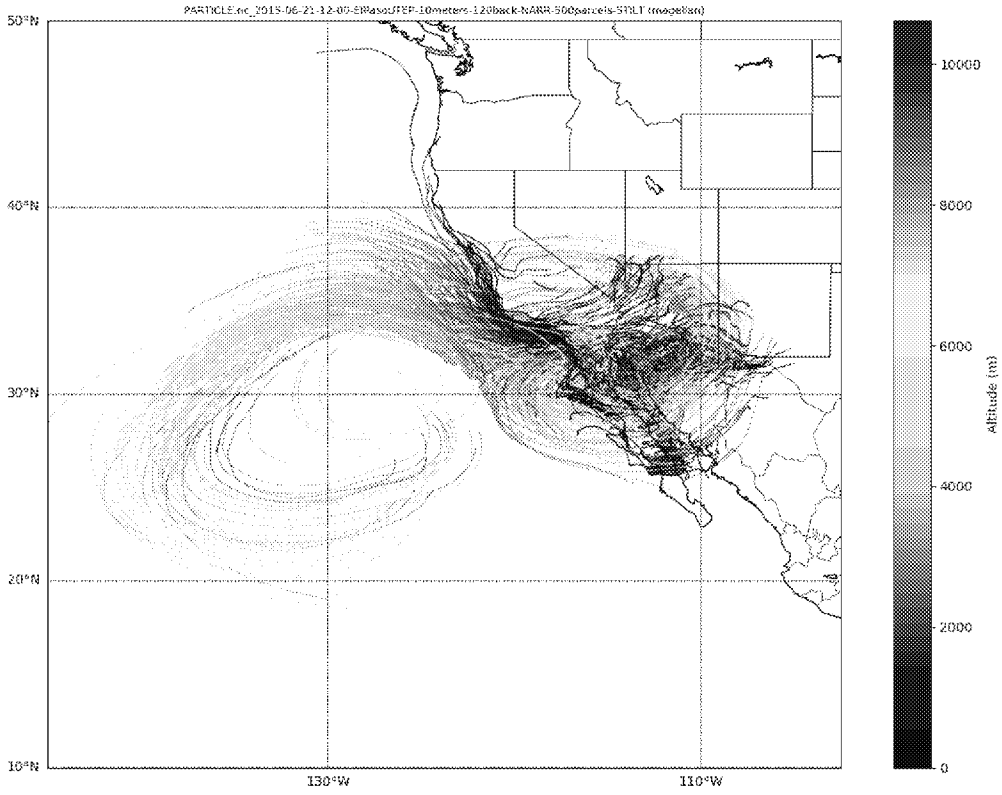

Figure 34: Five-day back trajectories for 500 parcels from the El Paso UTEP monitoring site (CAMS12) in El Paso-Juárez on June 21, 2015 at 12:00 UTC.

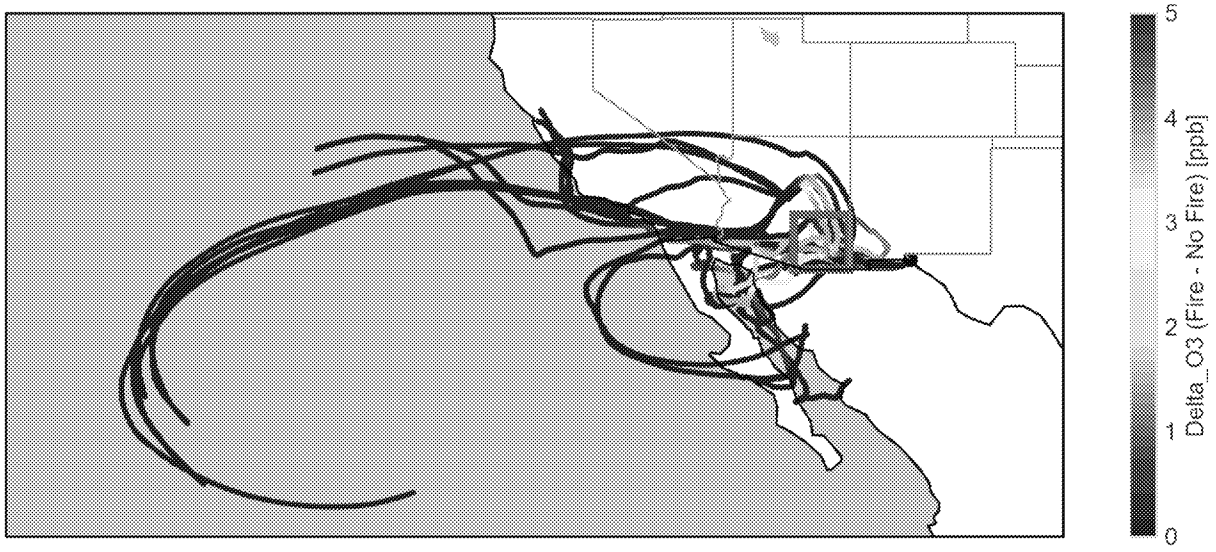

Figure 35: Five-day back trajectories for parcels from the El Paso UTEP monitoring site on June 21, 2015 that pass through the Southeastern Arizona fire region (red box) and have a fire-influenced ozone value (Delta_O3, color bar) of at least 1 ppbv during some part of the back trajectory. Of the 500 back-trajectories, 484 pass over the Southeastern Arizona fire region and 20 of those exceed 1 ppbv.

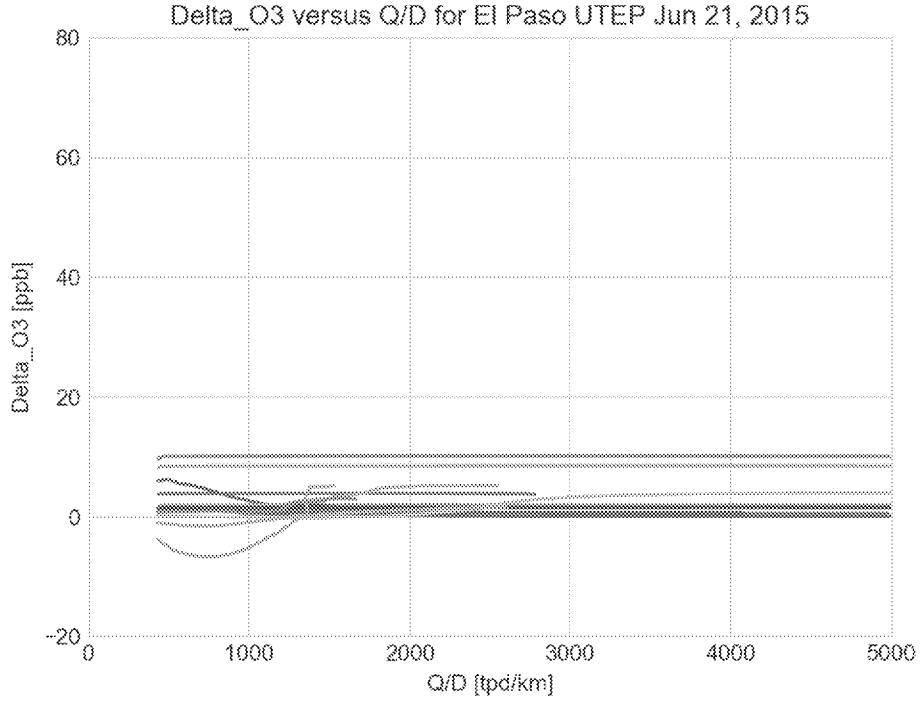

Figure 36: Plot for the El Paso UTEP site for June 21, 2015 of the fire-influenced ozone enhancement (Delta_O3, y-axis) versus the Q/D metric for the parcels that pass through the Southeastern Arizona fire region and have a fire-influenced ozone value (Delta_O3) of at least 1 ppbv during some part of the back trajectory. Of the 500 back-trajectories, 484 pass over the Southeastern Arizona fire region and 20 of those exceed 1 ppbv. The distances used to calculate

the D in the Q/D metric follow the parcel trajectories from the closest pass to the center of the Southeastern Arizona fire region to El Paso UTEP site. The colors of each back-trajectory are arbitrary.

5 Alternate Biomass Burning Screening Metrics

Our results in Sections 2-4 show that the Q/D metric is not consistent with either the literature or model simulations of the formation of O_3 in biomass burning plumes. This is due to the fact that O_3 is not directly emitted by the fire, but instead is formed during the oxidation of the NO_x and VOCs emitted by the fire over a period of hours to days, corresponding to distances of 100s of km. Thus O_3 impacts from fires generally increase with distance from the fire for a period of time before the effects of dilution take over to reduce the O_3 impacts at long distances unless fire NO_x is regenerated by the thermal decomposition of PAN. This plume-dominated chemistry can also be perturbed by the addition of anthropogenic NO_x when the fire passes over a city, which can lead to a second rapid O_3 production period.

In proposing alternate biomass burning metrics for Tier 2 screening for the impacts of fire on O_3, we focus mainly on the O_3 produced initially by the oxidation of the NO_x and VOCs emitted by the fire over a period of hours to a few days. Accounting for the impacts of PAN decomposition and anthropogenic NO_x would have to be done in a Tier 3 demonstration using photochemical models. Additionally, as the Tier 2 demonstration already requires the calculation of back-trajectories to determine that the monitor in question was actually impacted by the fires, that back-trajectory information could be incorporated into the screening metric itself. We also want our metric to be directly related to the published literature on O_3 formation in biomass burning plumes, and to be able to adjust as our knowledge improves. We also need a metric that accounts for the low NO_x to VOC ratios, and thus low O_3 formation, in boreal forest fires, and thus differentiates them from other fires in screening for impacts on O_3.

One literature-based approach would be to use the mean ratio between the O_3 enhancement and the CO enhancement in biomass burning plumes from review of Jaffe and Wigder (2013) as the basis of a screening metric. They estimate that biomass burning plume aged 1-2 days generally have a ratio of 0.2 $\pm$ 0.1 mol O_3/mol CO. Our ASP and STILT-ASP simualtions are generally consistent with this ratio (e.g., Lonsdale et al., 2017) for all fires except boreal forest fires, where a smaller literature value for this ratio could be used, such as the ARCTAS analysis of Alvarado et al. (2010), which obtained a ratio of 0.005 $\pm$ 0.019 mol O_3/mol CO for fresh boreal plumes. The STILT-ASP back-trajectories are already combined with fire emission inventories to estimate the impact of fires on CO without needing to have the computational expense or complication of calculating the photochemistry, and the CO impact of the fires from STILT-ASP can be multiplied by the ratios above to obtain an estimate of the O_3 impact of the fires. Thus the level of effort required for a Tier 2 demonstration with this metric would not be appreciably larger than what is already required for the Q/D plus back-trajectory approach.

One potential criticism of this screening metric is that CO is not directly involved in the production of O_3, so a metric that depends on the emissions of CO does not seem reasonable for a O_3 screening metric. In this case, as O_3 production in biomass burning is NO_x limited, we can instead use literature values for the ratio of the O_3 enhancement to the NO_y enhancement in biomass burning plumes, which may also directly account for the lower impacts of boreal forest fire plumes due to their lower NO_y emissions. Again, the fire impacts on NO_y can be estimated using STILT-ASP without photochemistry.

Another concern would be that our model results show that areas within ~100 km of a fire can have smaller impacts of fires on O_3 than areas further downwind. For these sources, a linear scale of the DO_3/DCO ratio from 0.0 at 0 km to the literature value at about 100 km downwind could be used to account for this effect.

6 Quality Assurance Steps and Reconciliation with User Requirements

All work on the project was done in accordance with the Quality Assurance Project Plan (QAPP). The source code, data files, and model output produced in this project were inspected by team members different from the original author to ensure they were correct, and any errors noted in early versions were fixed. Other required analyses are presented in the main report (Sections 3 and 4). In addition, if further analysis or feedback from TCEQ uncovers any errors in the provided files, we will correct those and provide TCEQ with corrected files as part of our Final Report.

The project Quality Assurance Project Plan (QAPP) listed several questions that needed to be addressed. These are addressed below:

- *Do the model predictions make physical sense given our conceptual models of O_3 precursor emissions, chemistry, and transport? Are there any unexplained features in the model results?*
  The ASP, STILT-ASP, and CAMx model predictions are all consistent with our conceptual models of O_3 formation in biomass burning plumes. In all the models there is initial rapid O_3 production due to the oxidation of fire NO_x and VOCs, with some evidence of additional production of O_3 as the fire VOCs mix with the anthropogenic NO_x in the El Paso-Ciudad Juárez region. The model results do not have significant unexplained features, but there are differences between the model approaches that could be subject to further investigation, as discussed below.

- *How sensitive are the model predictions to errors in the fire emission database?*
  While a full sensitivity study of the STILT-ASP and CAMx model results to errors in the fire emission database is outside of the scope of this project, we assessed the impact of these uncertainties by running the ASP Lagrangian parcel model for the Yucatan and Hog fire cases with different emission estimates, giving different initial concentrations for the box model simulations. As fire emission inventories can disagree by a factor of 2 or more, our estimates of the emissions covered a range of a factor of 4 (e.g., ΔCO_{init} from 75 ppbv to 300 ppbv for the Yucatan plume). The O_3 impacts were roughly proportional to the change in ΔCO_{init}, which suggests that errors in the fire emission databases in terms of the total amount of biomass burned have a roughly proportional impact on the model estimates of the O_3 impact on biomass burning.

- *Are the STILT-ASP back-trajectories reasonable?*
  The back-trajectories calculated with STILT-ASP (using NARR meteorology) are reasonable and are consistent with previous analyses of the HGB and El Paso events. Similar to the GEOS-Chem simulations of Prof. Yuxuan Wang of the University of Houston, we find that fire emissions from the Yucatan significantly impacted the HGB urban area on April 26, 2011 and May 1-2, 2013 (Section 3.2). However, STILT-ASP does suggest that there was no impact of Yucatan fires on April 27, 2011, as the back-trajectories for that day pass over the western US, and the simulations for the other days show a complex mix of air masses from northern Mexico and the southern US. For the June 21, 2015 El Paso event, the STILT-ASP back trajectories agree with the CAMx output and the HYSPLIT back-trajectories from the TCEQ exceptional event demonstration report in showing a significant impact from fires in Arizona, mainly the Hog Fire and Whitetail Fire

(Section 4.3). However, only a small percentage of the back-trajectories actually passed over the fire locations.

- *Are the different model predictions of the impact of biomass burning on O_3 consistent with each other, and with the scientific literature?*
  The model results are all consistent in showing that the Q/D metric does not correctly represent the dependence of fire O_3 enhancements with distance, and this is consistent with the scientific literature. However, they do disagree on the exact value of the fire O_3 enhancements in El Paso. The ASP simulations tend to predict larger values for these enhancements due to the use of cloud-free photolysis rates, no O_3 deposition, and no formation of organic nitrates by S/IVOC chemistry. The STILT-ASP simulations do include the effects of clouds on photolysis, O_3 deposition, and the formation of organic nitrates by S/IVOC chemistry, and thus predict lower values of the O_3 enhancements. The CAMx results are in between the two Lagrangian approaches. Further research is needed to determine which approach is more accurate and how the ASP, CAMx, and STILT-ASP models need to be adjusted to better represent the true O_3 enhancements in biomass burning plumes.

- *How well are the different model predictions of the impact of biomass burning emissions on O_3 approximated by the Q/D screening metric?*
  All of the model predictions suggest problems with the Q/D metric, as all three models predict that the impact of fire emissions on O_3 increases with distance from the fire on scales of ~100-1000 km downwind (Sections 3 and 4), which is consistent with the literature on the formation of ozone in biomass burning plumes (Section 2). This means that, for example, a city 300 km from a fire could have a higher impact of the fire on O_3 concentrations than a city within 100 km of the fire, which is the exact opposite of the behavior assumed in the Q/D metric. When this is combined with the fact that the threshold value of the Q/D metric is likely to exclude many moderate-sized fires that are more than 100 km away, this means that the Q/D metric could unintentionally allow a weaker threshold of evidence to be used for cities where the model-predicted O_3 impact is small and then require stricter evidence for cities further downwind where the models would suggest stronger O_3 impacts.

7 Conclusions

Here we summarize the conclusions of our project, with reference to the corresponding report section.

- Wildfires have a demonstrable impact on surface ozone within the US, although the highly variable meteorology and non-linear ozone chemistry make quantifying the impacts difficult. While many wildfires do impact surface ozone and do cause exceedances of air quality standards, not every fire does and the presence of a nearby wildfire is not in itself sufficient to prove wildfire impact on surface ozone (Section 2).
- Multiple publications show that given the right meteorological conditions (e.g. temperature, solar radiation, winds) and the right chemical conditions (e.g. high rVOC wildfire plumes and a source of reactive nitrogen), dramatic spikes in surface ozone levels can occur. Other publications demonstrate that there are other conditions in which a wildfire plume does not impact or influence surface ozone concentrations (Section 2).
- While the Q/D metric is a useful tool for identifying the *possibility* of wildfire influence on ozone enhancement events, it is perhaps too conservative of a metric. There are many examples in the literature of wildfire events impacting ozone concentrations that would fall outside of the Q/D metric's 100 tpd/km threshold, which highlights the non-linear nature of ozone photochemistry. It would only be for the most obvious wildfire events (very nearby the receptor, or exceptionally large events) that the Q/D metric would allow for a Tier 2 level of evidence. For the most part, air quality managers would be required to present the more-stringent Tier 3 level of evidence (Section 2).
- The ASP simulations generally show O_3 increasing with time and distance downwind over the two-day time frame simulated, and were thus inconsistent with the Q/D metric. However, the O_3 produced did increase somewhat proportionally with initial emissions if other parameters (e.g., mixing height, fire area) are held constant. While the O_3 formation at the end of two days is similar for fires with similar initial CO concentrations from grassland/savannah, tropical forest, and temperate forest fires, the O_3 formation from boreal forest fires is much lower, suggesting that different metrics are needed for screening O_3 impacts from boreal biomass burning fires (Sections 3.1 and 4.2).
- The STILT-ASP simulations showed O_3 production within individual parcels frequently increased with increasing distance, which is inconsistent with the Q/D metric. In addition, the meandering back-trajectories calculated by STILT-ASP show the limits of using a straight-line distance as a proxy for the travel distance of the fire plume (Sections 3.2 and 4.3). While some parcels follow straight-line trajectories and demonstrate significant O_3 enhancement due to wildfire emissions and follow relatively straight-line trajectories (e.g. Figure 14c), there are many more particles that show little-to-no ozone enhancement (and even ozone suppression) and meandering trajectories (e.g. Figure 14a).
- Using the GAMs for the HGB urban area to estimate fire impacts was not very effective, as the GAM model residuals during these events (+3-4 ppbv) are well within the standard error of the GAMs (~10 ppbv), and thus it is unclear if the residuals are due to fires or simply due to the random errors that are unavoidable in statistical models (Section 3.3).
- Analysis of the CAMx results for the El Paso exceptional event shows that the CAMx-simulated impacts of biomass burning on MDA8 O_3 on this day are not consistent with the Q/D metric. Instead, the fire impacts on MDA8 O_3 tend to increase with distance within 200-300 km of the fire, with some evidence of the Hog fire having additional O_3 production

due to interaction with the anthropogenic NO_x in the El Paso-Ciudad Juárez urban area. This dependence on distance is qualitatively consistent with the ASP and STILT-ASP model results (Section 4.1).

- Instead of the Q/D metric, we recommend a literature-based approach that uses literature ratios of O_3 enhancement by fires to the enhancement of CO and/or NO_y in the plumes. STILT-ASP back-trajectories can be used to estimate the impact of fires on CO and/or NO_y without needing to have the computational expense or complication of calculating the photochemistry. Thus the level of effort required for a Tier 2 demonstration with this approach would not be appreciably larger than what is already required for the Q/D plus back-trajectory approach (Section 5).

8 Recommendations for Further Study

We recommend that future work on the formation of O_3 in biomass burning plumes and their impacts on urban areas in Texas focus on:

- Using models to separate the O_3 formation within the biomass burning plume itself from the O_3 production caused by the mixing of biomass burning VOCs with anthropogenic NO_x in urban areas.
- Improving the chemistry in 3D Eulerian regional air quality models like CAMx and CMAQ to better represent the chemistry of biomass burning VOCs, including their formation of O_3, organic nitrates, and secondary organic aerosol (SOA).
- Parameterizing O_3 formation in biomass burning plumes using model emulators and other techniques to rapidly estimate the impacts of fires on a given urban area.
- Improvements to the STILT-ASP model, including better representation of plume rise, mixing among parcels, and deposition.

9 References

Akagi, S. K., Yokelson, R. J., Wiedinmyer, C., Alvarado, M. J., Reid, J. S., Karl, T., et al. (2011). Emission factors for open and domestic biomass burning for use in atmospheric models. *Atmospheric Chemistry and Physics*, *11*(9), 4039–4072. https://doi.org/10.5194/acp-11-4039-2011.

Akagi, S. K., Craven, J. S., Taylor, J. W., McMeeking, G. R., Yokelson, R. J., Burling, I. R., & Urbanski, S. P. (2012). Evolution of trace gases and particles emitted by a chaparral fire in California. *Atmos. Chem. Phys.*, *12*, 1397–1421. https://doi.org/10.5194/acp-12-1397-2012.

Akagi, S. K., Yokelson, R. J., Burling, I. R., Meinard+i, S., Simpson, I., Blake, D. R., et al. (2013). Measurements of reactive trace gases and variable O3formation rates in some South Carolina biomass burning plumes. *Atmospheric Chemistry and Physics*, *13*(3), 1141–1165. https://doi.org/10.5194/acp-13-1141-2013.

Alvarado, M. J., Logan, J. A., Mao, J., Apel, E., Riemer, D., Blake, D., et al. (2010). Nitrogen oxides and PAN in plumes from boreal fires during ARCTAS-B and their impact on ozone: An integrated analysis of aircraft and satellite observations. *Atmospheric Chemistry and Physics*, *10*(20), 9739–9760. https://doi.org/10.5194/acp-10-9739-2010.

Alvarado, M. J., Lonsdale, C. R., Yokelson, R. J., Akagi, S. K., Coe, H., Craven, J. S., et al. (2015). Investigating the links between ozone and organic aerosol chemistry in a biomass burning plume from a prescribed fire in California chaparral. *Atmospheric Chemistry and Physics*, *15*(12), 6667–6688. https://doi.org/10.5194/acp-15-6667-2015.

Alvarado, M., Brodowski, C., and Lonsdale, C. (2016). An Analysis of Biomass Burning Impacts on Texas, Final Report. Prepared by Atmospheric and Environmental Research (AER) for the Texas Commission on Environmental Quality (TCEQ).

Ambrose, J. L., Reidmiller, D. R., & Jaffe, D. A. (2011). Causes of high O3 in the lower free troposphere over the Pacific Northwest as observed at the Mt. Bachelor Observatory. *Atmospheric Environment*, *45*(30), 5302–5315. https://doi.org/10.1016/j.atmosenv.2011.06.056.

Andreae, M. O., & Merlet, P. (2001). Emission of trace gases and aerosols from biomass burning. *Global Biogeochemical Cycles*, *15*(4), 955–966.

Apel, E. C., Hornbrook, R. S., hills, A. J., Black, N.J., et al. (2015). Upper tropospheric ozone production from lightning NOx-impacted convection: Smoke ingestion case study from the DC3 campaign, J. Geophys. Res. Atmos., 120, 2505–2523, doi:10.1002/ 2014JD022121.

Baker, K. R., Woody, M. C., Tonnesen, G. S., Hutzell, W., Pye, H. O. T., Beaver, M. R., et al. (2016). Contribution of regional-scale fire events to ozone and PM2.5air quality estimated by photochemical modeling approaches. *Atmospheric Environment*, *140*, 539–554. https://doi.org/10.1016/j.atmosenv.2016.06.032.

Baylon, P., Jaffe, D. A., Wigder, N. L., Gao, H., & Hee, J. (2015). Ozone enhancement in western US wildfire plumes at the Mt. Bachelor Observatory: The role of NO_X. *Atmospheric Environment*, *109*, 297–304. https://doi.org/10.1016/j.atmosenv.2014.09.013.

Baylon, P., Jaffe, D. A., Hall, S. R., Ullmann, K., Alvarado, M. J., & Lefer, B. L. (2018). Impact of Biomass Burning Plumes on Photolysis Rates and Ozone Formation at the Mount Bachelor Observatory. *Journal of Geophysical Research: Atmospheres*, *123*(4), 2272–2284. https://doi.org/10.1002/2017JD027341.

Bein, K. J., Zhao, Y., Johnston, M. V., & Wexler, A. S. (2008). Interactions between boreal wildfire and urban emissions. *Journal of Geophysical Research Atmospheres*, *113*(7), 1–17. https://doi.org/10.1029/2007JD008910.

Bertschi, I. T., Jaffe, D. A., Jaeglé, L., Price, H. U., & Dennison, J. B. (2004). PHOBEA/ITCT 2002 airborne observations of transpacific transport of ozone, CO, volatile organic compounds, and aerosols to the northeast Pacific: Impacts of Asian anthropogenic and Siberian boreal fire emissions. *Journal of Geophysical Research D: Atmospheres*, *109*(23), 1–16. https://doi.org/10.1029/2003JD004328.

Brey, S. J., & Fischer, E. V. (2016). Smoke in the City: How Often and Where Does Smoke Impact Summertime Ozone in the United States? *Environmental Science and Technology*, *50*(3), 1288–1294. https://doi.org/10.1021/acs.est.5b05218.

Briggs, N. L., Jaffe, D. A., Gao, H., Hee, J. R., Baylon, P. M., Zhang, Q., et al. (2016). Particulate matter, ozone, and nitrogen species in aged wildfire plumes observed at the Mount Bachelor Observatory. *Aerosol and Air Quality Research*, *16*(12), 3075–3087. https://doi.org/10.4209/aaqr.2016.03.0120.

Bytnerowicz, A., Burley, J. D., Cisneros, R., Preisler, H. K., Schilling, S., Schweizer, D., et al. (2013). Surface ozone at the Devils Postpile National Monument receptor site during low and high wildland fire years. *Atmospheric Environment*, *65*, 129–141. https://doi.org/10.1016/j.atmosenv.2012.10.024.

Bytnerowicz, A., Hsu, Y. M., Percy, K., Legge, A., Fenn, M. E., Schilling, S., et al. (2016). Ground-level air pollution changes during a boreal wildland mega-fire. *Science of the Total Environment*, *572*(3), 755–769. https://doi.org/10.1016/j.scitotenv.2016.07.052.

Cahoon, D. R., Stocks, B. J., Levine, J. S., Cofer, W. R., & Pierson, J. M. (1994). Satellite analysis of the severe 1987 forest fires in northern China and southeastern Siberia. *Journal of Geophysical Research*, *99*(D9), 18627. https://doi.org/10.1029/94JD01024.

Chen, J., Li, C., Ristovski, Z., Milic, A., Gu, Y., Islam, M. S., et al. (2017). A review of biomass burning: Emissions and impacts on air quality, health and climate in China. *Science of the Total Environment*, *579*, 1000–1034. https://doi.org/10.1016/j.scitotenv.2016.11.025.

Cofer III, W. R., Levine, J. S., Winstead, E. L., Stocks, B. J., Cahoon, D. R., and Pinto, J. P. Trace gas emissions from tropical biomass fires: Yucatan peninsula, Mexico, Atmos. Environ., 27a, 1903–1907, 1993.

Craig, K., Alrick, D., Du, Y., Erdakos, G., MacDonald, C., Gross, T., and Watson, D. (2013). Use of Photochemical Grid Modeling to Quantify Ozone Impacts From Fires In Support Of Exceptional Event Demonstrations. Presented at the 12th Annual CMAS Conference, Chapel Hill, NC.

Crutzen, P. J., Heidt, L. E., Krasnec, J. P., Pollock, W. H., & Seiler, W. (1979). Biomass burning as a source of atmospheric gases CO, H2, N2O, NO, CH3Cl and COS. *Nature*, *282*, 253–256. https://doi.org/10.1038/282253a0

Daskalakis, N., Myriokefalitakis, S., & Kanakidou, M. (2015). Sensitivity of tropospheric loads and lifetimes of short lived pollutants to fire emissions. *Atmospheric Chemistry and Physics*, *15*(6), 3543–3563. https://doi.org/10.5194/acp-15-3543-2015

Dreessen, J., Sullivan, J., & Delgado, R. (2016). Observations and impacts of transported Canadian wildfire smoke on ozone and aerosol air quality in the Maryland region on June 9–12, 2015. *Journal of the Air and Waste Management Association*, *66*(9), 842–862. https://doi.org/10.1080/10962247.2016.1161674

Fine, R., Miller, M. B., Burley, J., Jaffe, D. A., Pierce, R. B., Lin, M., & Gustin, M. S. (2015). Variability and sources of surface ozone at rural sites in Nevada, USA: Results from two years of the Nevada Rural Ozone Initiative. *Science of the Total Environment*, *530–531*, 471–482. https://doi.org/10.1016/j.scitotenv.2014.12.027

Fiore, A. M., Pierce, R. B., Dickerson, R. R., & Lin, M. (2014). Detecting and attributing episodic high background ozone events. *EM: Air and Waste Management Association's Magazine for Environmental Managers*, 22–28.

Fischer, E.V., Jaffe, D.A., Reidmiller, D.R., and Jaegle, L. (2010). Meteorological controls on observed peroxyacetyl nitrate at Mount Bachelor during the spring of 2008. Journal of Geophysical Research 115, D03302.

Gifford, F. A. (1981). Horizontal Diffusion in the Atmosphere: A Lagrangian-Dynamical Theory. Los Alamos Scientific Laboratory, Report #LA-8667-MS, available at http://permalink.lanl.gov/object/tr?what=info:lanl-repo/lareport/LA-08667-MS.

Gong, X., Kaulfus, A., Nair, U., & Jaffe, D. A. (2017). Quantifying O $_3$ Impacts in Urban Areas Due to Wildfires Using a Generalized Additive Model. *Environmental Science & Technology*, *51*(22), 13216–13223. https://doi.org/10.1021/acs.est.7b03130

Goode, J. G., Yokelson, R. J., Susott, R. A., & Ward, D. E. (1999). Trace gas emissions from laboratory biomass fires measured by open-path Fourier transform infrared spectroscopy: Fires in grass and surface fuels. *Journal of Geophysical Research: Atmospheres*, *104*(D17), 21237–21245. https://doi.org/10.1029/1999JD900360

Jacob, D. J., & Winner, D. A. (2009). Effect of climate change on air quality. *Atmospheric Environment*, *43*, 51–63. https://doi.org/10.1016/j.atmosenv.2008.09.051.

Jaffe, D., Bertschi, I., Jaeglé, L., Novelli, P., Reid, J. S., Tanimoto, H., et al. (2004). Long-range transport of Siberian biomass burning emissions and impact on surface ozone in western North America. *Geophysical Research Letters*, *31*(16), 6–9. https://doi.org/10.1029/2004GL020093.

Jaffe, D., Chand, D., Hafner, W., Westerling, A., & Spracklen, D. (2008). Influence of fires on O3 concentrations in the western U.S. *Environmental Science and Technology*, *42*(16), 5885–5891. https://doi.org/10.1021/es800084k.

Jaffe, D. (2011). Relationship between Surface and Free Tropospheric Ozone in the Western U.S. *Environmental Science & Technology*, *45*(2), 432–438. https://doi.org/10.1021/es1028102.

Jaffe, D. A., & Wigder, N. L. (2012). Ozone production from wildfires: A critical review. *Atmospheric Environment*, *51*, 1–10. https://doi.org/10.1016/j.atmosenv.2011.11.063

Jaffe, D. A., Wigder, N., Downey, N., Pfister, G., Boynard, A., & Reid, S. B. (2013). Impact of Wild fi res on Ozone Exceptional Events in the Western U.S. *Environmental Science and Technology*, *47*, 11065–11072.

Junquera, V., Russell, M. M., Vizuete, W., Kimura, Y., & Allen, D. (2005). Wildfires in eastern Texas in August and September 2000: Emissions, aircraft measurements, and impact on photochemistry. *Atmospheric Environment*, *39*(27), 4983–4996. https://doi.org/10.1016/j.atmosenv.2005.05.004.

Lacaux, J. P., Delmas, R., & Jambert, C. (1996). NO_x emissions from African savanna fires in the form of litter. The experimental. *October*, *101*, 585–595.

Landis, M. S., Edgerton, E. S., White, E. M., Wentworth, G. R., Sullivan, A. P., & Dillner, A. M. (2018). The impact of the 2016 Fort McMurray Horse River Wildfire on ambient air pollution levels in the Athabasca Oil Sands Region, Alberta, Canada. *Science of the Total Environment*, *618*, 1665–1676. https://doi.org/10.1016/j.scitotenv.2017.10.008

Langford, A. O., Pierce, R. B., & Schultz, P. J. (2015). Stratospheric intrusions, the Santa Ana winds, and wildland fires in Southern California. *Geophysical Research Letters*, *42*(14), 6091–6097. https://doi.org/10.1002/2015GL064964

Lei, W., Li, G., & Molina, L. T. (2013). Modeling the impacts of biomass burning on air quality in and around Mexico City. *Atmospheric Chemistry and Physics*, *13*(5), 2299–2319. https://doi.org/10.5194/acp-13-2299-2013

Levine, J.S. Biomass Burning: The Cycling of Gases and Particulates from the Biosphere to the Atmosphere. (2014). Reference Module in Earth Systems and Environmental Sciences, Treatise on Geochemistry (Second Edition), Volume 5, 139-150.

Lin, M., Horowitz, L. W., Payton, R., Fiore, A. M., & Tonnesen, G. (2017). US surface ozone trends and extremes from 1980 to 2014: Quantifying the roles of rising Asian emissions, domestic controls, wildfires, and climate. *Atmospheric Chemistry and Physics*, *17*(4), 2943–2970. https://doi.org/10.5194/acp-17-2943-2017

Lindaas, J., Farmer, D. K., Pollack, I. B., Abeleira, A., Flocke, F., Roscioli, R., et al. (2017). Changes in ozone and precursors during two aged wildfire smoke events in the Colorado Front Range in summer 2015. *Atmospheric Chemistry and Physics*, *17*(17), 10691–10707. https://doi.org/10.5194/acp-17-10691-2017

Liu, X., Huey, L. G., Yokelson, R. J., Selimovic, V., Simpson, I. J., Müller, M., et al. (2017). Airborne measurements of western U.S. wildfire emissions: Comparison with prescribed burning and air quality implications. *Journal of Geophysical Research*, *122*(11), 6108–6129. https://doi.org/10.1002/2016JD026315.

Lobert, J. M. and Warnatz, J. (1993). Emissions from combustion processes in vegetation, from Fire in the Environment: The Ecological, Atmospheric, and Climatic Importance of Vegetation Fires, Ed: Cruzten, P.J., and Goldhammer, J.G.

Lu, X., Zhang, L., Yue, X., Zhang, J., Jaffe, D. A., Stohl, A., et al. (2016). Wildfire influences on the variability and trend of summer surface ozone in the mountainous western United States. *Atmospheric Chemistry and Physics*, *16*(22), 14687–14702. https://doi.org/10.5194/acp-16-14687-2016.

Mallia, D. V, Lin, J. C., Urbanski, S., Ehleringer, J., & Nehrkorn, T. (2015). Impacts of upwind wildfire emissions on CO, CO 2, and PM 2.5 concentrations in Salt Lake City, Utah. *Journal of Geophysical Research Atmospheres*, *120*, 147–166. https://doi.org/10.1002/2014JD022472.

Mao, J., Horowitz, L. W., Naik, V., Fan, S., Liu, J., & Fiore, A. M. (2013). Sensitivity of tropospheric oxidants to biomass burning emissions: Implications for radiative forcing. *Geophysical Research Letters*, *40*(6), 1241–1246. https://doi.org/10.1002/grl.50210.

Mauzerall, D. L., Logan, J. A., Jacob, D. J., Anderson, B. E., Blake, D. R., Bradshaw, J. D., et al. (1998). Photochemistry in biomass burning plumes and implications for tropospheric ozone over the tropical South Atlantic. *Journal of Geophysical Research: Atmospheres*, *103*(D7), 8401–8423. https://doi.org/10.1029/97JD02612.

McKeen, S. A., Wotawa, G., Parrish, D. D., Holloway, J. S., Buhr, M. P., Hübler, G., et al. (2002). Ozone production from Canadian wildfires during June and July of 1995. *Journal of Geophysical Research Atmospheres*, *107*(14), 1–25. https://doi.org/10.1029/2001JD000697.

Morris, G. A., Hersey, S., Thompson, A. M., Pawson, S., Nielsen, J. E., Colarco, P. R., et al. (2006). Alaskan and Canadian forest fires exacerbate ozone pollution over Houston, Texas, on 19 and 20 July 2004. *Journal of Geophysical Research Atmospheres*, *111*(24), 2–11. https://doi.org/10.1029/2006JD007090.

Nassar, R., Logan, J. A., Megretskaia, I. A., Murray, L. T., Zhang, L., & Jones, D. B. A. (2009). Analysis of tropical tropospheric ozone, carbon monoxide, and water vapor during the 2006

El Niño using TES observations and the GEOS-Chem model. *Journal of Geophysical Research Atmospheres*, *114*(17), 1–23. https://doi.org/10.1029/2009JD011760

Pfister, G. G., Emmons, L. K., Hess, P. G., Honrath, R., Lamarque, J. F., Val Martin, M., et al. (2006). Ozone production from the 2004 North American boreal fires. *Journal of Geophysical Research Atmospheres*, *111*(24), 1–13. https://doi.org/10.1029/2006JD007695.

Pfister, G. G., Wiedinmyer, C., & Emmons, L. K. (2008). Impacts of the fall 2007 California wildfires on surface ozone: Integrating local observations with global model simulations. *Geophysical Research Letters*, *35*(19), 1–5. https://doi.org/10.1029/2008GL034747.

Raffuse, S., Du, Y., Larkin, N., Lahm, P., 2012. Development of the 2008 wildland fire national emissions inventory. In: 20th International Emissions Inventory Conference, August, pp. 13-16.

Real, E., Law, K. S., Weinzierl, B., Fiebig, M., Petzold, A., Wild, O., et al. (2007). Processes influencing ozone levels in Alaskan forest fire plumes during long-range transport over the North Atlantic. *Journal of Geophysical Research Atmospheres*, *112*(10), 1–19. https://doi.org/10.1029/2006JD007576.

Singh, H. B., Cai, C., Kaduwela, A., Weinheimer, A., & Wisthaler, A. (2012). Interactions of fire emissions and urban pollution over California: Ozone formation and air quality simulations. *Atmospheric Environment*, *56*, 45–51. https://doi.org/10.1016/j.atmosenv.2012.03.046.

Tanimoto, H., Matsumoto, K., & Uematsu, M. (2008). Ozone-CO Correlations in Siberian Wildfire Plumes Observed at Rishiri Island. *Sola*, *4*(Supplement 1), 65–68. https://doi.org/10.2151/sola.2008-017.

TCEQ (2016). *June 21, 2015 Exceptional Event Demonstration Package For The El Paso County Maintenance Area.* Dated September 30, 2016.

Turquety, S., Logan, J. A., Jacob, D. J., Hudman, R. C., Leung, F. Y., Heald, C. L., et al. (2007). Inventory of boreal fire emissions for North America in 2004: Importance of peat burning and pyroconvective injection. *Journal of Geophysical Research Atmospheres*, *112*(12), 1–13. https://doi.org/10.1029/2006JD007281.

Urbanski, S. P. (2013). Combustion efficiency and emission factors for wildfire-season fires in mixed conifer forests of the northern Rocky Mountains, US. *Atmospheric Chemistry and Physics*, *13*(14), 7241–7262. https://doi.org/10.5194/acp-13-7241-2013.

Val Martín, M., Honrath, R. E., Owen, R. C., Pfister, G., Fialho, P., & Barata, F. (2006). Significant enhancements of nitrogen oxides, black carbon, and ozone in the North Atlantic lower free troposphere resulting from North American boreal wildfires. *Journal of Geophysical Research Atmospheres*, *111*(23), 1–17. https://doi.org/10.1029/2006JD007530.

van der Werf, G. R., Randerson, J. T., Giglio, L., Collatz, G. J., Mu, M., Kasibhatla, P. S., et al. (2010). Global fire emissions and the contribution of deforestation, savanna, forest, agricultural, and peat fires (1997–2009). *Atmospheric Chemistry and Physics*, *10*(23), 11707–11735. https://doi.org/10.5194/acp-10-11707-2010.

VanCuren, R. (Tony), & Gustin, M. S. (2015). Identification of sources contributing to PM2.5and ozone at elevated sites in the western U.S. by receptor analysis: Lassen Volcanic National Park, California, and Great Basin National Park, Nevada. *Science of the Total Environment*, *530–531*, 505–518. https://doi.org/10.1016/j.scitotenv.2015.03.091.

Verma, S., Worden, J., Pierre, B., Jones, D. B. A., Al-Saadi, J., Boersma, F., et al. (2009). Ozone production in boreal fire smoke plumes using observations from the Tropospheric Emission Spectrometer and the Ozone Monitoring Instrument. *Journal of Geophysical Research Atmospheres*, *114*(2). https://doi.org/10.1029/2008JD010108.

Voulgarakis, A., & Field, R. D. (2015). Fire Influences on Atmospheric Composition, Air Quality and Climate. *Current Pollution Reports*, *1*(2), 70–81. https://doi.org/10.1007/s40726-015-0007-z.

Voulgarakis, A.M., E. Marlier, G. Faluvegi, D. T. Shindell, K. Tsigaridis, and S. Mangeon (2015). Interannual variability of tropospheric trace gases and aerosols: The role of biomass burning emissions, J. Geophys. Res. Atmos., 120, 7157–7173, doi:10.1002/2014JD022926.

Ward, D. S., Shevliakova, E., Malyshev, S., & Rabin, S. (2018). Trends and Variability of Global Fire Emissions Due to Historical Anthropogenic Activities. *Global Biogeochemical Cycles*, *32*(1), 122–142. https://doi.org/10.1002/2017GB005787.

Wentworth, G. R., Aklilu, Y. Abeba, Landis, M. S., & Hsu, Y. M. (2018). Impacts of a large boreal wildfire on ground level atmospheric concentrations of PAHs, VOCs and ozone. *Atmospheric Environment*, *178*, 19–30. https://doi.org/10.1016/j.atmosenv.2018.01.013.

Wiedinmyer, C., S. K. Akagi, R. J. Yokelson, L. K. Emmons, J. A. Al-Saadi, J. J. Orlando, & A. J. Soja (2011). The Fire Inventory from NCAR (FINN), A high resolution global model to estimate the emissions from open burning. *Geosci. Model Dev., 4*, 625–641.

Wigder, N. L., Jaffe, D. A., & Saketa, F. A. (2013). Ozone and particulate matter enhancements from regional wildfires observed at Mount Bachelor during 2004-2011. *Atmospheric Environment*, *75*, 24–31. https://doi.org/10.1016/j.atmosenv.2013.04.026.

Wu, Y., Peña, W., Gross, B., & Moshary, F. (2018). Wildfire Smoke Transport and Impact on Air Quality Observed by a Multi-Wavelength Elastic-Raman Lidar and Ceilometer in New York City. *EPJ Web of Conferences*, *176*(05044).

Yates, E. L., Iraci, L. T., Singh, H. B., Tanaka, T., Roby, M. C., Hamill, P., et al. (2016). Airborne measurements and emission estimates of greenhouse gases and other trace constituents from the 2013 California Yosemite Rim wildfire. *Atmospheric Environment*, *127*, 293–302. https://doi.org/10.1016/j.atmosenv.2015.12.038.

Yates, E. L., Johnson, M. S., Iraci, L. T., Ryoo, J.-M., Pierce, R. B., Cullis, P. D., et al. (2017). An assessment of ground-level and free-tropospheric ozone over California and Nevada. *Journal of Geophysical Research: Atmospheres*, 89–102. https://doi.org/10.1002/2016JD026266.

Yokelson, R. J., Crounse, J. D., Decarlo, P. F., Karl, T., Urbanski, S., Atlas, E., et al. (2009). Emissions from biomass burning in the Yucatan. *Atmos. Chem. Phys.*, *9*, 5785–5812.

Young, P. J., Naik, V., Fiore, A. M., Gaudel, A., Guo, J., Lin, M. Y., et al. (2018). Tropospheric Ozone Assessment Report (TOAR): Assessment of global-scale model performance for global and regional ozone distributions, variability, and trends. *Elementa: Science of the Anthropocene*, *6*, 0–84. https://doi.org/10.1525/elementa.265.

Zhang, L., Jacob, D. J., Yue, X., Downey, N. V., Wood, D. A., & Blewitt, D. (2014). Sources contributing to background surface ozone in the US Intermountain West. *Atmospheric Chemistry and Physics*, *14*(11), 5295–5309. https://doi.org/10.5194/acp-14-5295-2014.

Zhang, L., & Jaffe, D. A. (2017). Trends and sources of ozone and sub-micron aerosols at the Mt. Bachelor Observatory (MBO) during 2004–2015. *Atmospheric Environment*, *165*, 143–154. https://doi.org/10.1016/j.atmosenv.2017.06.042.

Zhou, S., Collier, S., Jaffe, D. A., Briggs, N. L., Hee, J., Iii, A. J. S., et al. (2017). Regional influence of wildfires on aerosol chemistry in the western US and insights into atmospheric aging of biomass burning organic aerosol. *Atmospheric Chemistry and Physics*, *17*(3), 2477–2493. https://doi.org/10.5194/acp-17-2477-2017.

Zoogman, P., Jacob, D. J., Chance, K., Liu, X., Lin, M., Fiore, A., & Travis, K. (2014). Monitoring high-ozone events in the US Intermountain West using TEMPO geostationary satellite

observations. *Atmospheric Chemistry and Physics*, *14*(12), 6261–6271. https://doi.org/10.5194/acp-14-6261-2014.

Appendix A: Summary of Biomass Burning Literature Reviewed

Here we briefly review a wider range of literature, including publications that we did not include in the analysis above. This literature review centered around the Jaffe and Wigder (2012) and Jaffe et al. (2013) publications, and includes publications these two papers cited, as well as publications that cited these two papers. An Excel spreadsheet summarizing the full literature review will be submitted along with this Technical Memo.

There are many review articles that did not provide sufficient estimates of Q, D, or wildfire impacts on ozone values, or did not identify specific wildfire events that would allow us to estimate our own values (e.g. Lobert and Warnatz, 1993; Jaffe et al., 2008; Bein et al., 2008; Bytnerowicz et al., 2013; Fiore et al., 2014; Voulgarakis and Field, 2015; Fine et al., 2015). Other studies had a focus primarily on young plume chemistry rather than ozone enhancement at sites downwind (e.g. Akagi et al., 2013). There are many publications that investigate a portion of the wildfire influence on ozone, but which focus on some region other than North America, such as Russia/Siberia (Jaffe et al., 2004), Africa (Lacaux et al., 1996), Asia and long-range Asian transport (Cahoon et al., 1994; Jaffe et al., 2004; Bertschi et al., 2004; Chen et al., 2017), the tropics (Mauzerall et al., 1998; Nassar et al., 2009), the full global scale (Crutzen et al., 1979; Pfister et al., 2006; van der Werf et al., 2010; Mao et al., 2013; Voulgarakis and Field, 2015; Lin et al., 2017; Young et al., 2018; Ward et al., 2018), or focus on tropospheric (e.g. Val Martin et al., 2006; Ambrose et al., 2011; Jaffe, 2011; Mao et al., 2013; Apel et al., 2015; Daskalakis et al., 2015; Voulgarakis et al., 2015; Yates et al., 2017) or stratospheric (Langford et al., 2015; Yates et al., 2017) phenomena.

Other publications focused primarily on the impact of wildfires on aerosols and non-ozone gas species (e.g. Alvarado et al., 2015; Mallia et al., 2015; Briggs et al., 2016; Zhou et al., 2017; Zhang and Jaffe, 2017; Wu et al., 2018), or reported results from laboratory analysis (Goode et al., 1999) or satellite observations (Zoogman et al., 2014) that did not directly examine ozone enhancement, or they reported long-term climate-scale trends and did not focus on individual wildfire events (e.g. Lu et al., 2016; Lin et al., 2017). There are many studies that identify biomass burning plumes, but do not attempt to identify the individual wildfires which emitted the plumes (e.g. Fischer et al., 2010; Ambrose et al., 2011; Wigder et al., 2013; Baylon et al., 2015, 2018; Briggs et al., 2016; Zhang and Jaffe, 2017).

While there were many studies that estimated the influence of wildfires on ozone, many of them did not estimate absolute emissions, but rather made estimates of the normalized excess mixing ratio (NEMR), the emission ratio (ER), the emission factor (EF), and the modified combustion efficiency (MCE) (Andrae and Merlet, 2001; Akagi et al., 2011, 2012, 2013; Urbanski, 2013; Alvarado et al., 2015; Briggs et al., 2016; Yates et al., 2015; Liu et al., 2017). When the impact on ozone was estimated, many studies estimated the ozone enhancement ratio relative to CO ($\Delta O_3/\Delta CO$) (Akagi et al., 2013; Wigder et al., 2013; Baker et al., 2016; Baylon et al., 2015, Briggs et al., 2016; Yates et al., 2015) or estimated the ozone production rate (Baylon et al., 2018). We include in our above analysis primarily publications that reported an estimate of the mixing ratio enhancement of ozone from wildfire sources.

BALD	CH3CN	HOCH2CHO
IC3H7NO3	Acetylene	GLY
IC4H9NO3	ACR	ACETOL
NBUTOL	ALD	ISOP
NC3H7NO3	API	KET
NRPOPOL	BEN	LIM
OLI	Butadiene	HC5
OLT	Butanal	MCR
PHE	i-Butane	MEOH
ROH	n-Butane	MVK
XYM	i-Butene	MEK
XYO	trans-2-Butene	MGLY
XYP	DIEN	CH3NO3
1-Butene	Ethane	MethylPropanal
2-Butenal	ETOH	HONO
cis-2-Butene	C2H5NO3	Propanal
Acetaldehyde	ETHE	Propane
Acetic_Acid	HCHO	Propene
Acetone	Formic_Acid	TOL
	FURAN	

Table A1: List of MOZART-4 species summed together to estimate rVOC from the FINN emissions. This estimate is then multiplied by 2 to account for unidentified NMOCs, following the suggested approach of Akagi et al. (2011).

Location	Latitude Range (°N)	Longitude Range (W)	Citaiton
Wallow	31.5 - 37	103 - 114	Baker et al. (2016)
Flint Hills	35 - 41	93 - 99	Baker et al. (2016)
Yucatan	17 - 23	86 - 93	Yorkelson et al. (2009)
Fort McMurray	55 - 59	104 - 110	Wentworth et al. (2018)
Mexico City	estimate taken from publicaiton		Lei et al. (2013)
Western Canada	54 - 61	100 - 111	Lindaas et al. (2017)
Western US	42 - 50	107 - 120	Lindaas et al. (2017)
Maryland	45 - 55	85 - 105	Dreessen et al. (2016)
Western US	44 - 50	108 - 122	Gong et al. (2017)
Western US	42 - 49	113 - 120	Liu et al. (2017)
Alaska and Canada	outside of range		Morris et al. (2006)

Table A2: Bounding boxes for estimates of wildfire Q-values from FINN emissions